AD-A047 611 ANALYTIC SCIENCES CORP READING MASS F/G 8/5
GEOFAST - A FAST GRAVIMETRIC ESTIMATION ALGORITHM.(U)
AUG 77 W G HELLER, K S TAIT, S W THOMAS F19628-76-C-0286
UNCLASSIFIED TASC-TR-1007-1-1 AFGL-TR-77-0195 NL

| OF |
AD
A047611

END
DATE
FILMED
-78
DDC

AFGL-TR-77-0195

12

GEOFAST – A FAST GRAVIMETRIC ESTIMATION ALGORITHM

Warren G. Heller
Kevin S. Tait
Stephen W. Thomas
The Analytic Sciences Corporation
Six Jacob Way
Reading, Massachusetts 01867

25 August 1977

Final Report for Period 26 July 1976 – 25 August 1977

Prepared For

AIR FORCE GEOPHYSICS LABORATORY
Air Force Systems Command
United States Air Force
Hanscom Air Force Base, Massachusetts 01731

UNCLASSIFIED

SECURITY CLASSIFICATION OF THIS PAGE (When Data Entered)

REPORT DOCUMENTATION PAGE	READ INSTRUCTIONS BEFORE COMPLETING FORM
1. REPORT NUMBER: AFGL-TR-77-0195	2. GOVT ACCESSION NO.: none
	3. RECIPIENT'S CATALOG NUMBER:
4. TITLE (and Subtitle): GEOFAST - A Fast Gravimetric Estimation Algorithm,	5. TYPE OF REPORT & PERIOD COVERED: Final Sept. 26 Jul 76 - 7/26-76 - 8/25/77, 25 Aug 77
	6. PERFORMING ORG. REPORT NUMBER: TASC-TR-1007-1-1
7. AUTHOR(s): Warren G. Heller, Kevin S. Tait, Stephen W. Thomas	8. CONTRACT OR GRANT NUMBER(s): F19628-76-C-0286
9. PERFORMING ORGANIZATION NAME AND ADDRESS: The Analytic Sciences Corporation, Six Jacob Way, Reading, Massachusetts 01867	10. PROGRAM ELEMENT, PROJECT, TASK AREA & WORK UNIT NUMBERS: 62101F, 76000301, 17 43
11. CONTROLLING OFFICE NAME AND ADDRESS: Air Force Geophysics Laboratory, Hanscom AFB, Massachusetts 01731, Monitor/George Hadgigeorge/LWG	12. REPORT DATE: 25 August 1977
	13. NUMBER OF PAGES: 66 (67 p.)
14. MONITORING AGENCY NAME & ADDRESS (if different from Controlling Office)	15. SECURITY CLASS. (of this report): UNCLASSIFIED
	15a. DECLASSIFICATION/DOWNGRADING SCHEDULE

16. DISTRIBUTION STATEMENT (of this Report)

Approved for Public Release - Distribution Unlimited

17. DISTRIBUTION STATEMENT (of the abstract entered in Block 20, if different from Report)

DDC RECEIVED DEC 14 1977 B

18. SUPPLEMENTARY NOTES

19. KEY WORDS (Continue on reverse side if necessary and identify by block number)

Gravity Disturbance, GEOFAST, Least-Squares Estimation, Multisensor, Frequency Domain, Efficient Computation, Geodesy, Collocation

20. ABSTRACT (Continue on reverse side if necessary and identify by block number)

A mathematical algorithm called GEOFAST which uses modern frequency domain estimation techniques is developed for estimating gravity quantities such as the undulation of the geoid and the gravity disturbance vector. GEOFAST removes a restriction associated with an earlier algorithm, namely that data tracks be significantly longer than the correlation distances of the gravity quantities being measured. In the new algorithm no restrictions are placed on data track length.

DD FORM 1 JAN 73 1473 EDITION OF 1 NOV 65 IS OBSOLETE

404 565

UNCLASSIFIED

SECURITY CLASSIFICATION OF THIS PAGE (When Data Entered)

FOREWORD

This report extends a previously-developed (Ref. 1) gravimetric estimation algorithm by removing a data length restriction associated with the earlier algorithm. The original method, which could efficiently process very large amounts of data, required that measurements be available over an interval much longer than the correlation distances* associated with the gravimetric quantities being measured. This restriction could be significant in problems where long correlation distances occur such as processing geoid height data.

In the current study modern signal processing theory involving discrete Fourier transforms is used to solve the finite length estimation problem. The result of the effort is an efficient algorithm particularly applicable to processing large quantities of data. The new algorithm is called GEOFAST, an acronym for Geodetic Fast Estimation.

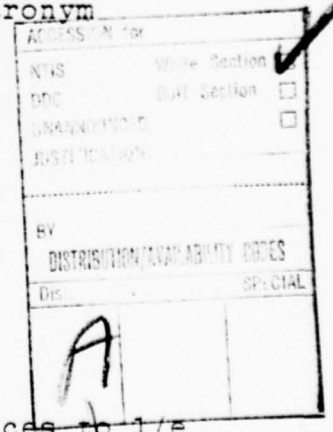

*Distance at which the autocovariance function reduces to 1/e of its value at zero shift.

TABLE OF CONTENTS

LIST OF FIGURES

1. INTRODUCTION

1.1 BACKGROUND

Continuing developments in gravimetric sensor technology are resulting in the availability of large amounts of gravity field data. In addition to greater densification of surface gravity measurements, large holdings of GEOS-3 satellite altimetric data are now available. Measurements of the ocean geoid will increase in abundance with the orbiting of SEASAT-A. The advent of moving-base gradiometry and utilization of satellite-to-satellite tracking measurements will add even more to the applicable data base.

The gravity field quantities which must be extracted from this heterogeneous data base are equally varied. Values of the gravity disturbance vector are needed to compensate terrestrial inertial navigation and guidance systems. Geoid undulations are needed for charting ocean currents and for determining elevation in geodetic surveys. Estimates of spatial derivatives of gravity are required for gravity gradiometer testing and evaluation. A schematic which illustrates examples of gravity field measurements of interest and lists some of the gravimetric quantities to be estimated from such measurements is presented in Fig. 1.1-1. These and other geophysical applications have the requirement for rapid, efficient gravimetric data processing.

Because of interrelations among all of the gravity field quantities, and because the value of the field at each point is significantly correlated with the gravity field at

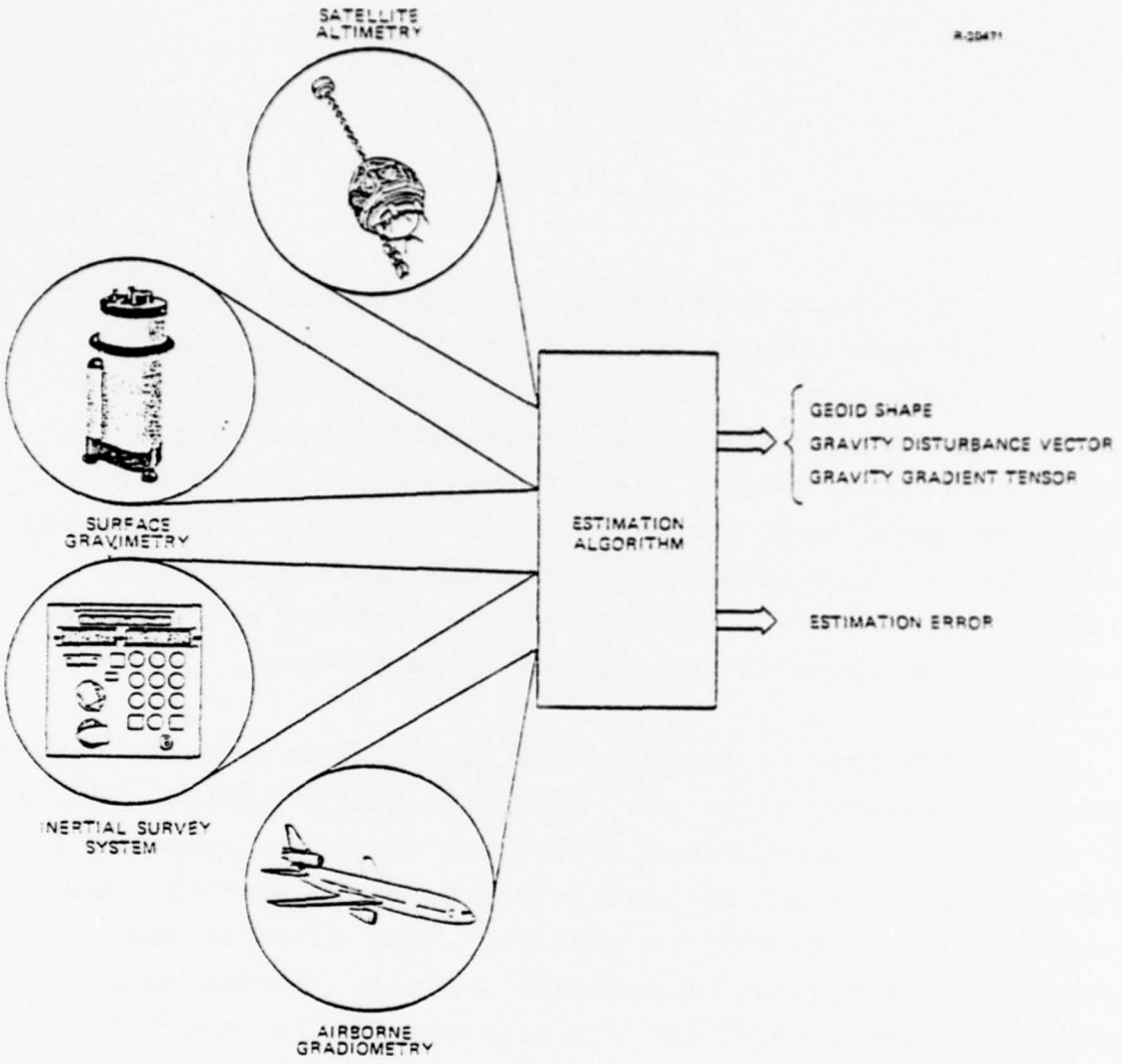

Figure 1.1-1 Gravimetric Sensors and Estimates

points considerably removed, it is possible to accurately predict values of gravimetric variables where little or no data exists. The techniques of classical geodesy (Ref. 2) provide formulas for making such inferences when noise-free data is available. For example, given gravity anomaly measurements over the entire Earth's surface, the disturbance potential is uniquely determined anywhere in space via Stokes' integral.

More recently, statistical techniques have been applied to optimally estimate gravity field quantities (Ref. 3) and, in many instances, have provided considerable advantage over classical methods (Refs. 4 and 7). One feature which makes the statistical approaches attractive is "built-in error analysis" which allows the impact of data deficiencies such as noise, discretization and finite extent to be easily studied. For some problems involving gravity effects along a single track (such as might be traversed by an inertially navigated terrestrial vehicle), recursive methods such as Kalman filtering have proved useful for processing large amounts of data (Ref. 5). However, the recursive approaches rely on state space formulations which are not easily applied to many gravimetric problems, particularly those which involve two or three dimensions. As a result, for most gravity quantity estimation problems, "classical" least squares techniques must be applied. Because such methods involve matrix inverses, excessive computational burdens result when a large number of measurement points is used (say 1000 or more). Of course a least squares estimation problem can always be truncated to reduce it to manageable size (e.g., Ref. 6), but the error involved in such approximations can be unacceptable. Evaluation of the error may also be difficult.

Another approach to least squares gravimetric data processing is developed in Ref. 1. The concept exploits the special structure of the gravity model covariance matrices instead of approximating either the data or the integral relations among gravimetric quantities. The formulation takes advantage of the computational efficiency of fast Fourier transforms and results in an estimation algorithm which is suitable for processing gravimetric data sets containing very large numbers of measurements (100,000 measurements provide

no difficulty). However, the algorithm developed in Ref. 1 is subject to moderate levels of error when the data interval is not significantly larger than the correlation distance of the gravity quantities being measured.

1.2 PURPOSE AND SCOPE OF THIS REPORT

In this report, further development of the frequency domain gravimetric estimation method developed in Ref. 1 is presented. In particular, the algorithm is extended to eliminate errors due to an approximation which neglects certain aspects of the finite length of data inputs. The enhanced algorithm, called GEOFAST (Geodetic Fast Estimation), is fully optimal* and still retains the necessary computational speed required to solve very high order gravimetric† estimation problems. Of course, as with any estimation technique, errors arising from finite, noisy data of limited extent still cause estimation errors. The merit of the estimation technique described in this report is that no computational errors are added in the course of processing the data.

GEOFAST fully and explicitly takes into account the finite range of data available from most gravimetric surveys without limiting the generality of problems to which the algorithm is applicable. Thus, the augmented algorithm is suited to multisensor gravimetric estimation problems (as well as those involving a single measured quantity) in exactly the same fashion as the earlier approach. Specifically, suitable

---

*Results in minimum variance of the estimation error when correct statistical gravimetric models are utilized.

†The term gravimetric is used in the broad sense of relating to techniques for measuring or estimating the gravitational disturbance potential or any of its derivatives.

data inputs include any gravimetric quantity available at gridpoints on or above the earth's surface. The purpose of this report is to describe enhancements to the frequency domain estimation algorithm of Ref. 1 which result in an optimal procedure for estimating gravimetric quantities from multisensor data.

In Chapter 2, the mathematical development of the algorithm is presented in some detail. Chapter 3 summarizes the enhanced algorithm and indicates the logical next steps for its exploitation. Recommendations for useful tests of GEOFAST are also presented.

1.3 TECHNICAL APPROACH

Minimum variance estimation as applied to gravimetric quantities is described in Ref. 1. Without repeating that discussion, it is appropriate to review the rationale for utilizing the frequency domain formulation, namely that the burden of manipulating large covariance matrices associated with the estimation process is eased. The discrete Fourier transformation takes advantage of the special structure of covariance matrices involved in the estimation problem. The matrices that require inversion in the discrete Fourier transform formulation are diagonal or band-diagonal. In the case of finite data lengths, the number of superdiagonal bands (and hence the computation effort required to effect a matrix inverse), is proportional to the sidelobe energy of the finite length data spectrum. To minimize this sidelobe energy, and thereby minimize the number of superdiagonal bands in the spectral density matrix, a data "window" is used. The GEOFAST algorithm consists of transforming the "windowed" data into the discrete frequency domain and there solving the

estimation equations using correspondingly windowed and transformed covariance functions. The actual solution of the banded-diagonal set of equations in the frequency domain is accomplished by the Cholesky decomposition technique. An overview of the complete approach is depicted in Fig. 1.3-1.

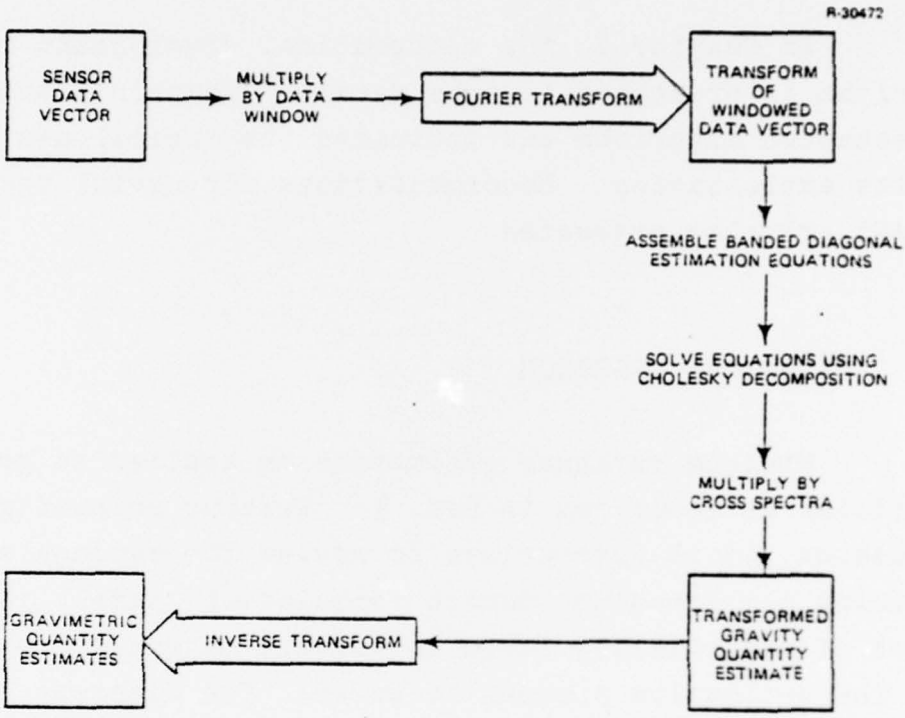

Figure 1.3-1 GEOFAST Algorithm

2. FAST COMPUTATIONAL METHODS FOR ESTIMATION

2.1 COMPUTATIONAL ELEMENTS OF GEOFAST

The various statistical procedures for gravimetric estimation have several mathematical operations in common. The most important example of such an operation is the solution of a system of equations involving the data covariance matrix. A second important operation is the vector-matrix multiplication typically carried out after solving the covariance equations. These straightforward algebraic operations are significant because of the large amounts of computer time they can require. For many large gravity quantity estimation problems, a conventional implementation of the estimation equations leads to prohibitive computer processing requirements. The computational load occurs primarily because standard algebraic algorithms do not take account of the special mathematical structure found in gravity quantity estimation problems. This chapter is concerned with fast computational methods for carrying out the fundamental mathematical operations in gravity quantity estimation. In particular a technique which exploits the special structure of the gravity estimation covariance matrices is developed.

The class of statistical procedures for gravity quantity estimation to which the techniques of this report are most applicable, has been called the "method of least squares collocation" (Ref. 3). This method utilizes minimum variance estimation for a model of the form

$$\underline{z} = H\underline{x} + \underline{v} \qquad (2.1\text{-}1)$$

where $\underline{z}$ is the data vector of observations, $\underline{x}$ is the vector of gravity quantities to be estimated, and $\underline{v}$ is the measurement noise vector. The vector $\underline{x}$ may consist partly of deterministic and partly of random variables which are related to the observations through the measurement matrix H.

Three special cases of the method are defined below. These cases are referred to as

- IMVE (implicit minimum variance estimation)
- BLUE (best least-squares unbiased estimation)
- EMVE (explicit minimum variance estimation)

If $\underline{x}$ is assumed to be a stochastic vector and H = I, where I is the unit matrix, then an estimation procedure is obtained which is referred to here as implicit minimum variance estimation (IMVE). The terminology emphasizes that the relation between $\underline{x}$ and $\underline{z}$ is given implicitly through a cross-covariance matrix C_{xz}. If $\underline{x}$ is assumed to be a deterministic vector and H defines an explicit (linearized) functional relation between $\underline{x}$ and $\underline{z}$, the procedure is termed best least-squares unbiased estimation (BLUE). This is simply another name for standard least-squares parameter estimation. Reference 3 shows that if $\underline{x}$ is partly stochastic and partly deterministic, the estimation procedure decouples into the two cases just defined. A third form of the method results if $\underline{x}$ is assumed to be stochastic, but related explicitly to $\underline{z}$ through the measurement matrix H. This case, which is designated explicit minimum variance estimation (EMVE), has been shown (Ref. 6), to be equivalent to the first case if $\underline{x}$ is given an a priori covariance matrix C_{xx} and the distribution of $\underline{z}$ is defined through Eq. 2.1-1. This case corresponds to a standard Kalman filter implementation (Ref. 19).

2.1.1 IMVE

The mathematical operations of IMVE are representative of those found in gravity quantity estimation in general. In this formulation (Ref. 1), the estimate vector, $\hat{\underline{x}}$, is found from the data vector, $\underline{z}$, via

$$\hat{\underline{x}} = C_{xz}\, C_{zz}^{-1}\, \underline{z} \qquad (2.1\text{-}2)$$

where C_{zz} and C_{xz} are covariance matrices obtained from a self-consistent statistical gravity model. If the dimensions of $\underline{x}$ and $\underline{z}$ are m and n, respectively, then C_{zz} and C_{xz} are respectively n×n and m×n matrices. The dimensionality of these two matrices, and their analogs in other formulations, is the source of the computational burden in estimation problems: for large n and m, the implementation of Eq. 2.1-2 requires very large amounts of computer time and is subject to severe processing errors. The calculation of the vector $C_{zz}^{-1}\, \underline{z}$ is the dominant part of this calculation. Efficient <u>general purpose</u> algorithms for this operation require, at the minimum, a number of numerical operations (multiplications and additions) which is approximately $n^3/3$. Table 2.1-1 illustrates the rapid growth of processing time with increasing data size that this cubic law produces. The operation which completes Eq. 2.1-2 is, of course, the multiplication of the vector $C_{zz}^{-1}\, \underline{z}$ by the cross-covariance matrix C_{xz}. Straightforward implementation of this operation requires mn multiplications and m(n-1) additions. When the number of quantities to be estimated, m, is small this operation is relatively inexpensive and may be carried out by standard algorithms. When m approaches or surpasses the order of n, a special purpose algorithm for covariance matrix multiplication can significantly reduce the cost of this operation. The first diagram in Fig. 2.1-1 illustrates the decomposition of Eq. 2.1-2 into the operations of covariance equation solution and covariance matrix multiplication.

TABLE 2.1-1

COMPUTATIONAL COST OF MINIMUM VARIANCE ESTIMATION

	DATA POINTS	OPTIMISTIC ESTIMATE OF PROCESSING TIME
SINGLE TRACK	1000	15 min
5 - TRACK	5000	30 hr
10 - TRACK	10000	10 days

2.1.2 EMVE and BLUE

The operations associated with the explicit measurement equation formulation of EMVE and with parametric BLUE are similar to those for IMVE. From Refs. 3 and 6, the expressions analogous to Eq. 2.1-2 are:

$$\text{(EMVE)} \quad \hat{\underline{x}} = (H^T C_{vv}^{-1} H + C_{xx}^{-1})^{-1} H^T C_{vv}^{-1} \underline{z} \qquad (2.1\text{-}3)$$

$$\text{(BLUE)} \quad \hat{\underline{x}} = (H^T C_{vv}^{-1} H)^{-1} H^T C_{vv}^{-1} \underline{z} \qquad (2.1\text{-}4)$$

where H is an n×m measurement matrix, C_{vv} is the n×n measurement noise covariance matrix, and C_{xx} is the m×m a priori covariance matrix for $\underline{x}$. The superscript, ^{T}, indicates matrix transpose.

Equations 2.1-3 and 2.1-4 may both be conveniently decomposed into three sequential operations:

- Computation of $\underline{a} = C_{vv}^{-1} \underline{z}$
- Multiplication to form $\underline{b} = H^T \underline{z}$
- Computation of $\hat{\underline{x}} = (H^T C_{vv}^{-1} H)^{-1} \underline{b}$, or $\hat{\underline{x}} = (H^T C^{-1} H + C_{xx}^{-1})^{-1} \underline{b}$

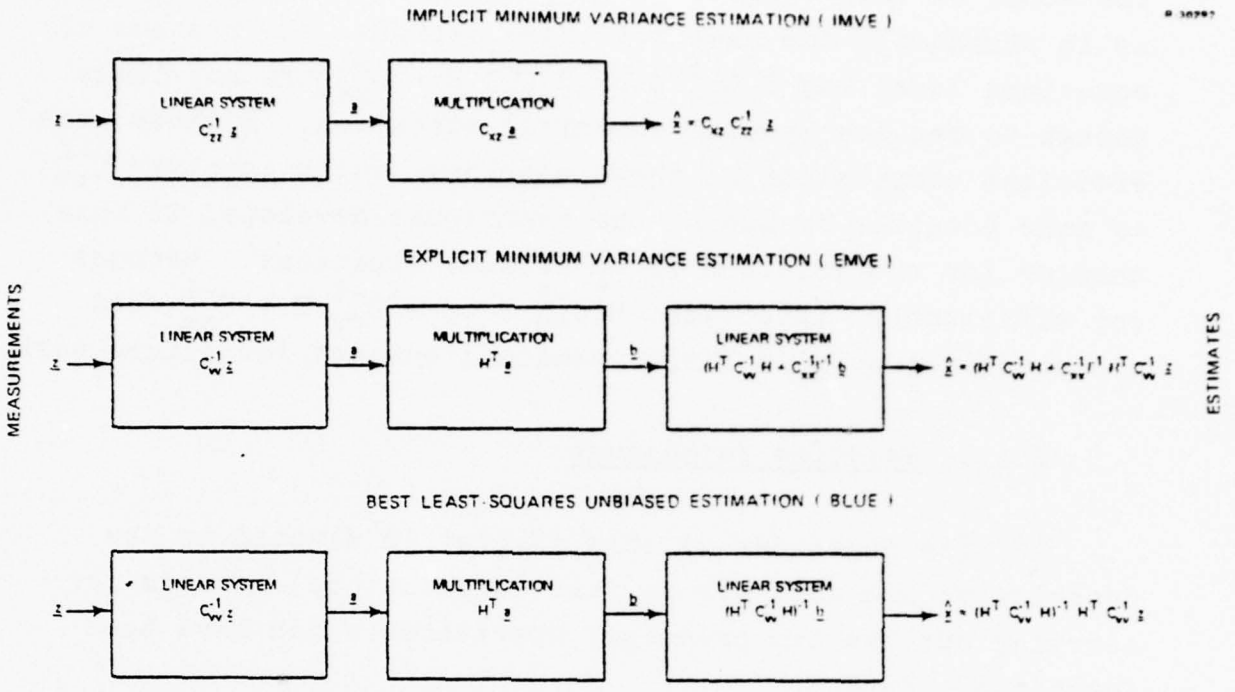

Figure 2.1-1 Block Diagrams of Gravimetric Estimation Algorithms

Block diagrams of the EMVE and BLUE processes are presented in Fig. 2.1-1. The first two of these operations are subject to the same considerations and the same special processing methods as are the operations of IMVE. However, for many problems C_{vv} is a diagonal matrix (although this is by no means always the case), so that the solution of the corresponding covariance equations is computationally inexpensive. When, in conjunction with diagonal C_{vv}, the dimension of $\underline{x}$ is not large, both the EMVE and BLUE method may be efficiently implemented without special attention to computationally fast methods.

Special computational methods for the third operation associated with the EMVE or BLUE procedures are outside

the scope of this report. When $\underline{x}$ is not of large dimension, as is ordinarily the case for these methods, the systems of equations involving $H^T C_{vv}^{-1} H$ or $H^T C_{vv}^{-1} H + C_{xx}^{-1}$ are not large enough to require special numerical attention. However, the efficient computation of these matrices, which involves C_{vv}^{-1}, is made possible by use of the techniques developed in this chapter for the solution of covariance equations. Methods for efficiently "inverting" $H^T C_{vv}^{-1} H$ or $H^T C_{vv}^{-1} H + C_{xx}^{-1}$ when the dimension of $\underline{x}$ is large, remain a subject for future work.

2.1.3 Solution Techniques

The remainder of this chapter is devoted to the description and analysis of fast computational methods for carrying out the two principal operations which have been identified above:

- Solution of large systems of equations involving C_{zz} or C_{vv}
- Fast multiplication of matrices C_{xz} or H when the dimension of $\underline{x}$ is large

The methods discussed in this chapter are those appropriate for gravity quantity estimation problems. Typically such problems entail stationary statistical models and an operator relating the various gravity quantities which does not change under spatial translations.

The method presented in the pages which follow for solution of stationary covariance equations is new, and is an extension of the classical frequency domain Wiener method. The basic approach of generalized Wiener filtering is described in Ref. 14 and depends for its success on the fast Fourier transform (FFT) technique (Ref. 15). The use

of classical Wiener filtering techniques in conjunction with gravity data processing has been discussed in Ref. 1. This report develops an extended computational technique which retains the speed of the Wiener method, and, at the same time, offers the high degree of accuracy required for gravity quantity estimation.

2.2 SPECTRAL REPRESENTATION OF TOEPLITZ MATRICES

The new computation methods about to be presented herein are based on so-called Toeplitz matrices (Ref. 16). Toeplitz matrices consist of a class of n×n, real-valued matrices which includes the covariance matrices from stationary random processes. More formally, a matrix T is of the Toeplitz type if there is a real-valued function, ϕ_ℓ, such that the elements of T obey

$$[T]_{jk} = \phi_{k-j}, \quad 0 \leq j, k \leq n-1 \tag{2.2-1}$$

If T is an autocovariance or a cross covariance matrix, then ϕ_ℓ is the corresponding covariance function. The matrix T is symmetric if the function ϕ_ℓ is even.

The relevance of Toeplitz matrices to statistical estimation has already been hinted at in the definition above. The covariance matrices (e.g., C_{xx}, C_{xz}, C_{zz}, C_{vv}) which appear in the various expressions for IMVE, EMVE, and BLUE are of the Toeplitz type when the underlying statistical models are stationary. In addition, for problems involving the estimation of gravity quantities, the measurement matrix H is either a Toeplitz matrix or a submatrix from a Toeplitz

matrix. This follows from the fact that the geopotential operators connecting the various gravity quantities such as the Stokes, Vening Meinsez, and upward continuation operators, are invariant under spatial shifts (see, for instance Ref. 21). Toeplitz matrices result when operators with this property are reduced to finite dimensions, typically by discretization and truncation. As a consequence of stationary gravity models and shift-invariant measurement operators, essentially all large matrices appearing in the gravity quantity estimation problem are of the Toeplitz type. The study of fast computational methods for gravity quantity estimation is largely the study of efficient methods to handle equations defined by Toeplitz matrices.

2.2.1 Fourier Transformation of Circulant Matrices

Circulant matrices are a subset of Toeplitz matrices with an especially simple form under Fourier transformation. A Toeplitz matrix is a circulant (Ref. 8), if the function ϕ_ℓ, defined by Eq. 2.2-1 obeys

$$\phi_{-\ell} = \phi_{n-\ell}, \quad \ell = 1, \ldots, n-1 \qquad (2.2\text{-}1)$$

Matrices with this property may be identified by the fact that each row is equal to the row preceding it shifted one element to the right, with the last element "wrapped around" to the first place. For example, a circulant matrix with the first row $(\phi_0, \phi_1, \ldots, \phi_{n-1})$ necessarily has its second row given by $(\phi_{n-1}, \phi_0, \phi_1, \ldots, \phi_{n-2})$. While circulant matrices themselves do not appear frequently, their properties are useful in dealing with the more general Toeplitz matrices.

Circulant matrices have the special property that they are diagonalized by the discrete Fourier transformation (DFT). The n dimensional DFT matrix F is the n×n, symmetric complex-valued matrix whose elements are*

$$[F]_{jk} = \frac{1}{\sqrt{n}} \exp - \frac{2\pi ijk}{n} , \quad 0 \leq j, k \leq n-1 \tag{2.2-3}$$

and its inverse is easily seen to be $F^{\dagger}$. The DFT of an n-vector of complex numbers, $\underline{x}$, is defined by the relations (Ref. 9)

$$\underline{X} = F\,\underline{x}, \quad \underline{x} = F^{\dagger}\underline{X} \tag{2.2-4}$$

The matrix similarity transformation corresponding to Eq. 2.2-4 is given by

$$C_{\omega} = FCF^{\dagger} \tag{2.2-5}$$

where C is an n×m matrix of complex numbers and C_{ω} is its representation in the Fourier transform domain. The usefulness of the circulant matrix definition depends largely on the following result.

The Fourier transformation, Eq. 2.2-5, of any circulant matrix C is the diagonal matrix

$$C_{\omega} = \sqrt{n}\ \mathrm{diag}(\phi_0, \ldots, \phi_{n-1}) \tag{2.2-6}$$

*The symbol i denotes $\sqrt{-1}$, and the superscript ($\dagger$) denotes the complex conjugate transpose.

where $\underline{\phi}$ is the discrete power spectrum

$$\underline{\phi} = (\phi_0, \ldots, \phi_{n-1})^T = F^+ \underline{\phi} \qquad (2.2\text{-}7)$$

and $\underline{\phi} = (\phi_0, \ldots, \phi_{n-1})^T$ corresponds to the first row of C. Moreover, any diagonal matrix is the Fourier transform of a circulant matrix, defined by Eqs. 2.2-6 and 2.2-7. If the matrix C is symmetric the inverse transform F^+ may be replaced by F in Eq. 2.2-7. A proof of this result may be found in Ref. 9. This theorem is also equivalent to the well known relationship between discrete convolutions and discrete Fourier transforms proved in Ref. 10.

2.2.2 Fast Toeplitz Matrix Multiplication

A computationally fast algorithm for multiplying a vector by a Toeplitz matrix may be obtained as a consequence of the circulant matrix result presented in Section 2.2.1. This method, together with the fast procedure for solving linear equations described in Section 2.3, are the major components of an efficient gravity quantity estimation algorithm. Together, the two algorithms provide a gravity data processing method with computer time requirements proportional to n log n, where n is the number of data points.

In gravity quantity estimation the need for an operation equivalent to multiplying a vector by a Toeplitz matrix (or a partition of a Toeplitz matrix) has been described in Section 2.1. The matrix to be multiplied is either the cross covariance matrix C_{xz} or the transpose of the measurement matrix, H^T. In both cases, the dimension of the matrix to be multiplied, which will be denoted here by T, is m×n where m is the dimension of the vector to be estimated and n is the dimension of the data vector. The computational cost of

carrying out this vector-matrix multiplication by standard means is, of course, mn (scalar) multiplications and m(n-1) additions. When m is small compared to n, an ordinary matrix multiplication procedure can be used without affecting the overall efficiency of the estimation algorithm. When m is an appreciable fraction of n, the cost of this simple operation may dominate the cost of the data processing procedure unless a special-purpose algorithm is used. Such an algorithm is presented below.

By assumption, the matrix to be multiplied, T, is a Toeplitz matrix or, when m<n, a partition of a Toeplitz matrix. It follows that the elements of T are of the form

$$[T]_{jk} = t_{k-j}; \quad 0 \leq j \leq m-1, \quad 0 \leq k \leq n-1 \tag{2.2-8}$$

where t_ℓ is the appropriate function. In the case that m<n, the matrix T must be extended so that it is a (square) Toeplitz matrix. This is accomplished by defining the n×n matrix $\tilde{T}$ by

$$[\tilde{T}]_{jk} = t_{k-j}; \quad 0 \leq j, k \leq n-1 \tag{2.2-9}$$

The multiplication of an arbitrary vector, say $\underline{b}$, by the Toeplitz matrix $\tilde{T}$ may now be carried out, with the first m elements of the result containing the desired product, $T\underline{b}$. The problem then is simply one of developing an efficient procedure for calculating $\tilde{T}\underline{b}$.

The means for fast multiplication of $\tilde{T}$ follows from the circulant theorem of Section 2.2.1. The matrix T can be imbedded in a 2n×2n circulant matrix C, as follows. The function t_ℓ is extended to the range $-(2n-1) \leq \ell \leq (2n-1)$ by the definition

$$c_\ell = \begin{cases} t_\ell, & 0 \le \ell \le n-1 \\ 0, & \ell = n \\ t_{\ell-2n}, & n+1 \le \ell \le 2n-1 \end{cases} \qquad (2.2\text{-}10)$$

and $c_{-\ell} = c_{2n-\ell}$ for $1 \le \ell \le 2n-1$. The matrix C with elements

$$[C]_{jk} = c_{k-j} \qquad (2.2\text{-}11)$$

is now a circulant. Moreover, the circulant C has the additional property that

$$C \begin{pmatrix} \underline{b} \\ \underline{0} \end{pmatrix} = \begin{pmatrix} \tilde{T}\underline{b} \\ \underline{d} \end{pmatrix} \qquad (2.2\text{-}12)$$

where $\underline{b}$ is an arbitrary n-vector and $\underline{0}$ is the zero vector of length n. The vector $\tilde{T}\underline{b}$ is the desired product vector, while the n-vector $\underline{d}$ is discarded. The result of Section 2.2.1 is applied to carry out the multiplication using fast Fourier transforms.

Define $\underline{B}$ and $\underline{\Phi}_c$ to be the transforms

$$\underline{B} = F\begin{pmatrix} \underline{b} \\ \underline{0} \end{pmatrix}, \qquad (2.2\text{-}13a)$$

$$\underline{\Phi}_c = F\underline{c} \qquad (2.2\text{-}13b)$$

with the elements

$$\underline{B} = \left(B_0, B_1, \ldots, B_{2n-1}\right)^T$$
$$\underline{\Phi}_c = \left(\Phi_0, \Phi_1, \ldots, \Phi_{2n-1}\right)^T \qquad (2.2\text{-}14)$$

Then from Eqs. 2.2-5 to 2.2-7 the vector

$$C_\omega \underline{B} = \sqrt{n}\left(\Phi_0 B_0,\ \Phi_1 B_1,\ \ldots,\ \Phi_{2n-1} B_{2n-1}\right)^T \qquad (2.2\text{-}15)$$

is the DFT of the product vector in Eq. 2.2-12. An application of the inverse Fourier transform, $F^\dagger$, produces the desired result. The overall algorithm for fast matrix multiplication is diagrammed in Fig. 2.2-1. The cost of the entire procedure is dominated by the cost of three applications of the Fast Fourier Transform algorithm, and is proportional to n log n.

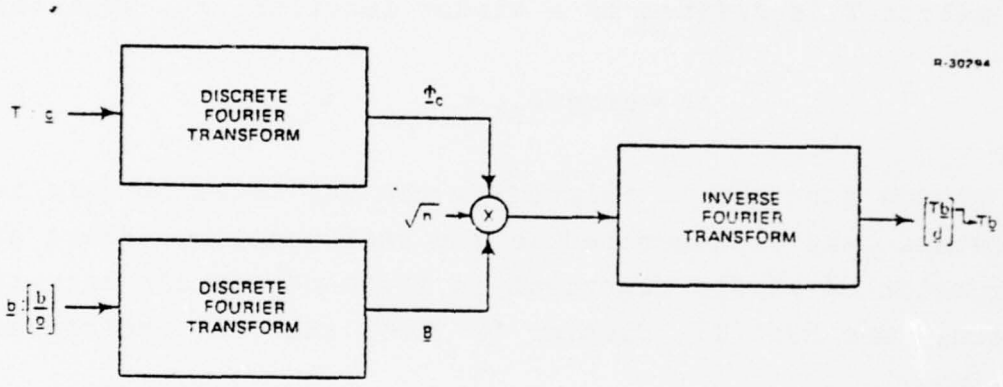

Figure 2.2-1 Overview of Fast Toeplitz Matrix Multiplication

Thus, the multiplication of a vector by a Toeplitz matrix is equivalent to the convolution of two discrete functions of finite length. The algorithm presented here for Toeplitz matrix multiplication is, in fact, equivalent to a well-known fast convolution algorithm, which has been described in Refs. 9 and 10.

2.2.3 The Transform of a General Toeplitz Matrix

In the algorithm presented in Section 2.3 for solving systems of equations, it will be necessary to calculate the Fourier transform of a Toeplitz matrix and of a "windowed" Toeplitz matrix. An algorithm for accomplishing this which involves approximately n log n computer operations is derived here from the result of Section 2.2.1. For the purposes of this section, a windowed Toeplitz matrix is one which has been multiplied by a diagonal matrix, W, to form

$$C = W\,T\,W \tag{2.2-16}$$

The matrix W is defined by a window function, w_ℓ, such that

$$W = \mathrm{diag}(w_0, w_1, \ldots, w_{n-1}) \tag{2.2-17}$$

The window function is related to the way in which data is processed, and is described in the next section. For a general discussion of window functions in frequency domain data processing, see Ref. 17, Chapter 3. Note that one choice for W is simply

$$W = I \tag{2.2-18}$$

where I is the n×n unit matrix. Thus, the class of windowed Toeplitz matrices includes all Toeplitz matrices.

The DFT of the windowed Toeplitz matrix in Eq. 2.2-16 is

$$T_\omega = FCF^{+} = FWTWF^{+} \tag{2.2-19}$$

The work of deriving a useful element-by-element expression for this matrix is divided into two parts: first, obtaining an expression for T_ω in terms of transforms of diagonal and circulant matrices and, second, applying the circulant theorem of Section 2.2.1 to deduce an efficient computational formula. The details of this derivation, which is central to the present technique, are provided in Appendix A.

The result is the expression*

$$\left[T_\omega\right]_{jk} = \sum_{\ell=0}^{2n-1} \Omega_{\ell-2j} \overline{\Omega}_{\ell-2k} \tau_\ell \qquad (2.2\text{-}20)$$

where the 2n dimensional vectors $\underline{\Omega}$ and $\underline{\tau}$ are defined as follows. The complex vector $\underline{\Omega}$ is the 2n dimensional transform**

$$\underline{\Omega} = \left(\Omega_0, \Omega_1, \ldots, \Omega_{2n-1}\right)^T = \frac{1}{\sqrt{2n}} F_{2n}^{\dagger} \begin{bmatrix} \underline{w} \\ \underline{0} \end{bmatrix} \qquad (2.2\text{-}21)$$

of the extended window function where

$$\underline{w} = \left(w_0, w_1, \ldots, w_{n-1}\right)^T \qquad (2.2\text{-}22)$$

The real vector $\underline{\tau}$ is the power spectrum corresponding to the extended circulant function c_ℓ defined in Eq. 2.2-10. That is, $\underline{\tau}$ is the 2n dimensional transform

$$\underline{\tau} = \left(\tau_0, \tau_1, \ldots, \tau_{2n-1}\right)^T = \sqrt{2n}\, F_{2n}\, \underline{c} \qquad (2.2\text{-}23)$$

---

* The notation $\overline{\Omega}_\ell$ represents the complex conjugate of the quantity Ω_ℓ.

**The 2n dimensional DFT matrix, F_{2n}, is defined by Eq. 2.2-3 with n replaced by 2n.

where

$$\underline{c} = \left(c_0, c_1, \ldots, c_{2n-1}\right)^T \qquad (2.2\text{-}24)$$

Equation 2.2-20 displays the elements of T_ω as weighted sums of a power spectrum $\underline{\tau}$, where the weights are determined by a spectral window $\underline{\Omega}$. Since T_ω can be interpreted as a frequency domain covariance matrix, Eq. 2.2.20 is analogous to the integral formulas which hold in the spectral representation of a stationary stochastic process (see, for example, Ref. 11, p. 200). The application of this formula for T_ω to the solution of the systems of equations encountered in gravity quantity estimation is described in the next section.

2.3 EFFICIENT SOLUTION OF COVARIANCE EQUATIONS

The requirement in gravity quantity estimation for an algorithm to solve large systems of equations with coefficients given by covariance matrices has been discussed in Section 2.1. The solution of such equation sets is the single most expensive operation in the estimation process. For problems involving large amounts of data, the use of standard algorithms for solving the covariance equations results in prohibitive computer time requirements. For gravity estimation problems, or any estimation problem involving stationary models, the covariance matrix defining the system of equations has a highly redundant, Toeplitz structure. The exploitation of this special mathematical structure makes it possible to greatly reduce the computer processing time required to solve the covariance equations. This increase in efficiency is reflected in a decrease, by orders of magnitude, in the processing time required for the solution of the overall estimation problem. This section presents a new highly efficient

algorithm for the solution of systems of equations with Toeplitz structure.

2.3.1 Algorithm Overview

The new GEOFAST algorithm is based on the transformation of the system of covariance equations into the frequency domain, and on the use of an appropriate data window to control the frequency domain matrix structure. Consider the solution of a system of equations

$$T\underline{u} = \underline{z} \tag{2.3-1}$$

where T is an n×n Toeplitz matrix. For the gravity quantity estimation problem, T represents the modeled data covariance matrix and $\underline{z}$ is the data vector. The vector $\underline{u}$ represents the solution vector required for subsequent stages of processing. Note that Eq. 2.3-1 may be solved using any convenient coordinate transformations. If a nonsingular transformation, A, is appropriately applied to $\underline{u}$ and $\underline{z}$ the equivalent system

$$T'\underline{u}' = \underline{z}' \tag{2.3-2a}$$

is obtained, where

$$T' = ATA^{\dagger}$$

$$\underline{u}' = (A^{\dagger})^{-1}\,\underline{u} \tag{2.3-2b}$$

$$\underline{z}' = A\underline{z}$$

Once Eq. 2.3-2 is solved, the solution vector $\underline{u}$ is simply found from

$$\underline{u} = A^{\dagger}\underline{u}' \tag{2.3-3}$$

Of course, the objective in carrying out such a transformation is to obtain a system of equations, Eq. 2.3-2, which is inexpensive to solve.

GEOFAST employs a transformation which is composed, first, of multiplication by a data window and, second, of application of the DFT. Multiplication by a data window is represented by an n×n diagonal matrix, defined by Eq. 2.2-17. The transformation A under consideration here is thus

$$A = FW \tag{2.3-4}$$

where F is the DFT matrix of Eq. 2.2-3. With this choice T' is identical to the matrix T_ω defined in Eq. 2.2-19. The main advantage of this transformation is that it can be made to give the matrix T' a very sparse structure, with only negligibly small elements outside a narrow band about the main diagonal. This special structure is discussed in detail in Section 2.3.2. A second important advantage of the windowed DFT is that it is very inexpensive to apply: windowing itself is a very simple operation, while the DFT can be carried out with the Fast Fourier Transform algorithm.

A block diagram for the overall algorithm is presented in Fig. 2.3-1. The transformation described by Eqs. 2.3-3 and 2.3-4 is used to produce a system of equations for which the matrix T' is very nearly band-diagonal. The matrix T' is then approximated by a matrix T_δ which is exactly band-diagonal and which differs from T' only in that it sets small out-of-band elements to zero. The system of equations, Eq. 2.3-2, is then solved with T' replaced by T_δ. The matrix T_δ has the band-diagonal structure

$$T_{\delta} = \begin{pmatrix} \overbrace{X \cdots X}^{M_B + 1} & & & 0 \\ & \ddots & & \\ & & \ddots & \\ X & & & X \\ & \ddots & & \\ & & \ddots & \\ 0 & & X \cdots & X \end{pmatrix} \Bigg\} M_B + 1 \qquad (2.3\text{-}5)$$

where all the elements of T_{δ} are zero except for those in a diagonal band consisting of the main diagonal and M_B sub- and superdiagonals. The difference between T' and T_{δ}, consisting of the out-of-band elements of T', can be made as small as desired by adjusting the data window and selecting an appropriate matrix bandwidth, M_B. The relationship between the data window and the size of the neglected elements is explored in Section 2.3.2.

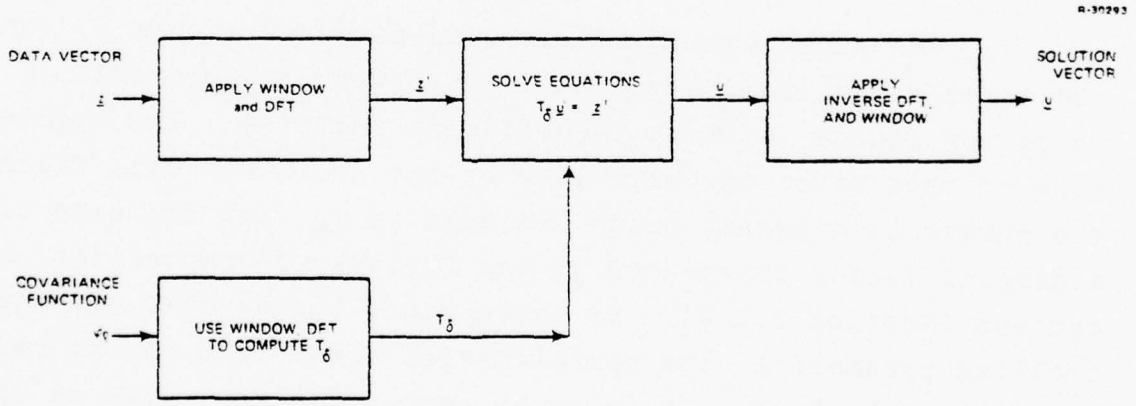

Figure 2.3-1 Overview of GEOFAST Algorithm

By applying the windowed DFT, the system of equations to be solved has been reduced to one with the band-diagonal matrix T_δ of Eq. 2.3-5. This is extremely advantageous because a band-diagonal system of this type, where M_B is much smaller than the dimension, n, of T_δ, can be solved in far fewer numerical operations than a full system. Application of the band-diagonal implementation of Cholesky decomposition (Ref. 12) requires numerical operations proportional to only $M_B^2 n$, as compared to n^3 for a full system. The results presented in Section 2.3.4 indicate that values of M_B on the order of 10 may be adequate for T_δ. For $M_B = 10$, the resulting reduction in computer processing time is proportional to $(n/10)^2$, which amounts to several orders of magnitude for large gravity quantity estimation problems. A consequence of the reduction of the system of equations, Eq. 2.3-1, to band-diagonal form is thus a substantial reduction in the amount of computer time required to obtain a solution.

The substitution of the band-diagonal matrix T_δ for the exactly transformed matrix T' involves an approximation which, of course, effects the solution vector $\underline{u}$. The magnitude of this error is controlled by the choice of data window, the number of diagonal bands included in T_δ, and the size of a damping factor introduced in the Cholesky decomposition process (Section 2.3.3). By appropriate choice of these controlling parameters, the approximation error in $\underline{u}$ can be made as small as desired. It is to be emphasized that what is being considered here is computational error in approximating T' with T_δ, rather than statistical error in computing an estimate from data. The statistical error is, of course, subject to the usual considerations, and not controlled in any way by the computational parameters discussed here. The computational error in the new algorithm and mechanisms for controlling it are analyzed in Section 2.3.3.

2.3.2 Computation of the Transformed Covariance Matrix

The computation of the transformed Toeplitz matrix, T_δ, is a major portion of the new algorithm. This part of the algorithm is particularly important for two reasons:

- The expression for T_δ shows how the data window determines matrix bandwidth.
- Special computational methods are required to keep the computer time required for generating the elements of T_δ to a minimum.

Both reasons make the formulas for the elements of T_δ and the manner in which they are implemented central to the overall algorithm.

As described in Section 2.3.1, the matrix T_δ is defined conceptually by applying a linear transformation given in Eq. 2.3-4 to the matrix T to obtain the matrix T' from Eq. 2.3-3, and setting to zero all elements of T' outside a predetermined bandwidth. The word "conceptually" is used here because the detailed algorithm, explained below, modifies the DFT matrix F shown in Eq. 2.3-4 to use only half of the frequencies present. It will become apparent that this modification simply eliminates the redundancy which occurs because the data are always real-valued. An expression for T', before any modification is made to F, is available directly from Section 2.2.3. Since $T'=T_\omega$ Eq. 2.2-20 provides

$$[T']_{k,k+m} = \sum_{\ell=0}^{2n-1} \Omega_{\ell-2k} \overline{\Omega}_{\ell-2(k+m)} \tau_\ell \qquad (2.3\text{-}6)$$

where the subscripts of the elements of T' have been arranged so that the elements

$$\left[T_\delta\right]_{k,k+m} \qquad 0 \leq k \leq n-m-1 \tag{2.3-7}$$

represent the m^{th} diagonal band. The functions Ω_ℓ and τ_ℓ are defined by Eq. 2.2-21 and 2.2-23 as described in Section 2.2.3.

The impact of the window function on the structure of T' can be seen from Eq. 2.3-6. The elements of the m^{th} diagonal band are obtained by convolving the power spectrum τ_ℓ with the weighting function.

$$\sigma_\ell(m) = \Omega_\ell \, \overline{\Omega}_{\ell-2m} \tag{2.3-8}$$

which consists of the transformed data window multiplied by its conjugate shifted 2m elements to the right.

Two typical window functions and their transforms are shown in Fig. 2.3-2. These windows are special cases of the Kaiser window function which has proved very useful in signal processing applications, and is defined in Refs. 17 and 18. Transforms of data windows are characterized by a mainlobe and a series of sidelobes of considerably reduced levels. As can be seen from Fig. 2.3-2, the disparity between mainlobe and sidelobe levels becomes more pronounced as the width of the mainlobe is increased. This behavior is reflected in the numerical structure of the matrix T'. The elements of T' corresponding to the shaded area of Fig. 2.3-3 cannot be neglected because the mainlobes of Ω_ℓ and $\Omega_{\ell-2m}$ overlap for these elements. However, the elements of T' outside the shaded area of the figure are the product of the sidelobes

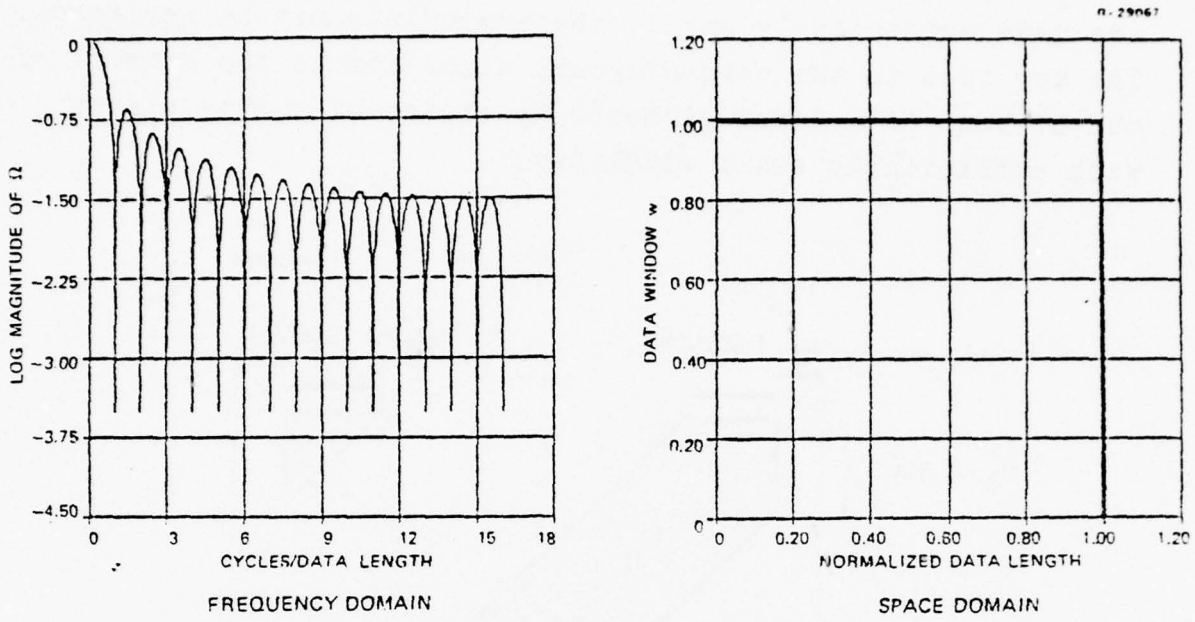

RECTANGULAR WINDOW: MAINLOBE WIDTH = 1

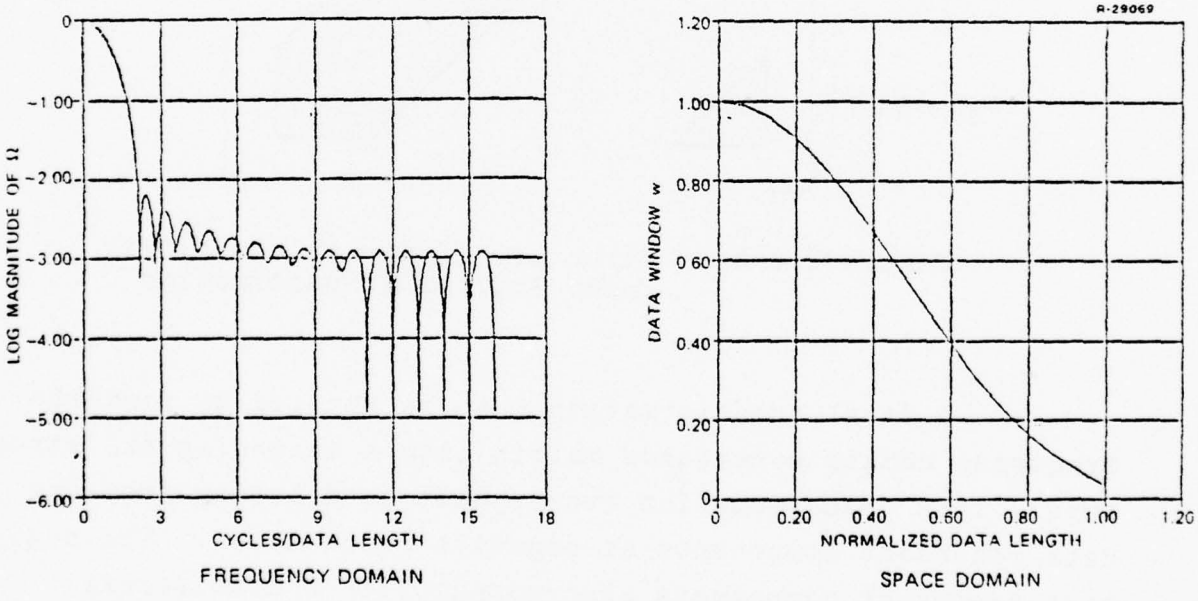

KAISER WINDOW: MAINLOBE WIDTH = 2

Figure 2.3-2 Data Windows and Transforms

of Ω_ℓ together with the power spectrum τ_ℓ. When the sidelobes are made sufficiently small, these elements may be neglected. The key idea in the band-diagonal algorithm is the control of out-of-band covariance elements by choice of a data window with sufficiently small sidelobes.

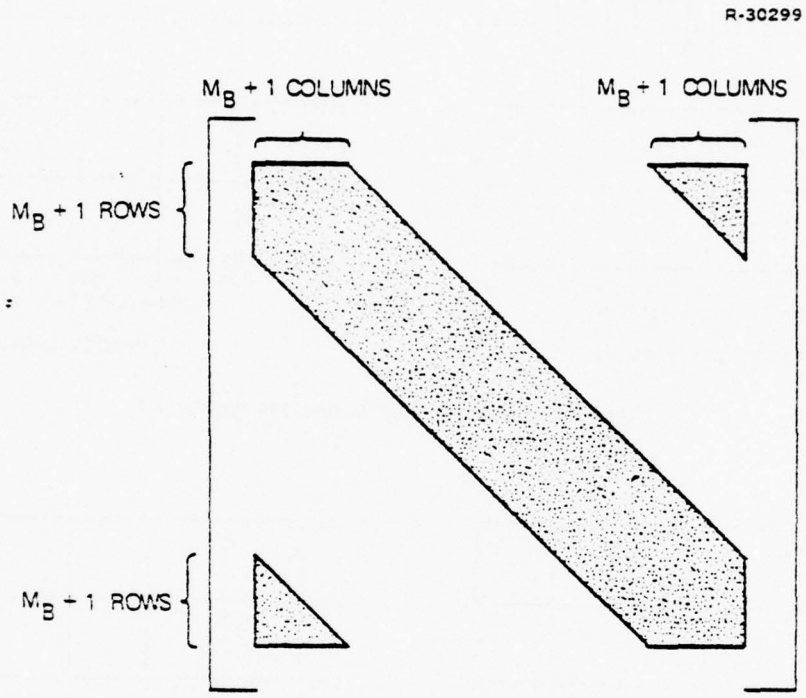

Figure 2.3-3 Structure of Covariance Matrix Under Fourier Transformation

A final transformation must be applied to form the frequency domain covariance matrix into a band-diagonal structure. This transformation corresponds to deleting from the data redundant components at negative frequencies. The negative frequency components are redundant in a statistical

sense because it is known that the data must always be real-valued. Put another way, the sine-cosine transform coefficients are sufficient to describe the data, rather than the full, complex set of Fourier coefficients. The practical importance of this last transformation is the elimination of the elements in the upper right and lower left corners of T' as shown in Fig. 2.3-3. With the elimination of these elements, a standard banded Cholesky algorithm may be used to solve the resulting system of covariance equations.

The transformation to sine-cosine coefficients corresponds to modifying the transformation matrix A of Eq. 2.3-3 to the form

$$A = HFW \tag{2.3-9}$$

where H is an n×n complex transformation from Fourier coefficients to sine-cosine coefficients. The elements of H are defined by

$$H = \frac{1}{\sqrt{n}} \begin{bmatrix} 2 & \overbrace{\quad}^{\frac{n}{2}-1} & \overbrace{\quad}^{\frac{n}{2}-1} \\ & 1 \;\ddots\; 1 & \\ & 1 \qquad 1 & \\ & 2 & \\ & i \;\ddots\; -i & \\ & i \qquad -i & \end{bmatrix} \begin{matrix} \\ \left.\begin{matrix} \\ \\ \end{matrix}\right\} \frac{n}{2}-1 \\ \\ \left.\begin{matrix} \\ \\ \end{matrix}\right\} \frac{n}{2}-1 \end{matrix} \tag{2.3-10}$$

The first n/2+1 rows of H generate the cosine coefficients of the data, while the last n/2-1 rows generate the sine coefficients. The result of applying the modified transformation, Eq. 2.3-9, to the definition of T' is shown in Fig. 2.3-4. The matrix T' is now a simple band-diagonal matrix, neglecting the small elements due to the sidelobes of Ω_ℓ. The sine-cosine transformation has two additional advantages:

- The nonzero elements of T' may be partitioned into blocks of dimension n/2+1 and n/2-1 corresponding to cosine and sine coefficients. The dimension of the largest system of equations to be solved is thus approximately halved.
- The elements of T' are real-valued eliminating the need for complex-valued numerical operations.

Other than these modifications, the banded structure of the transformed covariance matrix is unaffected by the introduction of H.

2.3.3 Algorithm Performance

The use of an appropriate data window gives the DFT of the covariance matrix a numerical structure which may be readily exploited in solving equations. The analysis of Section 2.3.2 shows that T_δ will have the band-diagonal form shown in Eq. 2.3-5 and Fig. 2.3-4. The matrix T_δ differs from the exact frequency domain covariance matrix T' only in that it neglects the very small elements which fall outside the diagonal band. A very efficient approximate solution to the covariance equations is found by replacing the exact matrix T' by T_δ in Eq. 2.3-2. The special structure of T is exploited by employing the band-diagonal implementation of the Cholesky decomposition algorithm (Ref. 12, Section 2.3) for the solution of linear equations. The resulting error in

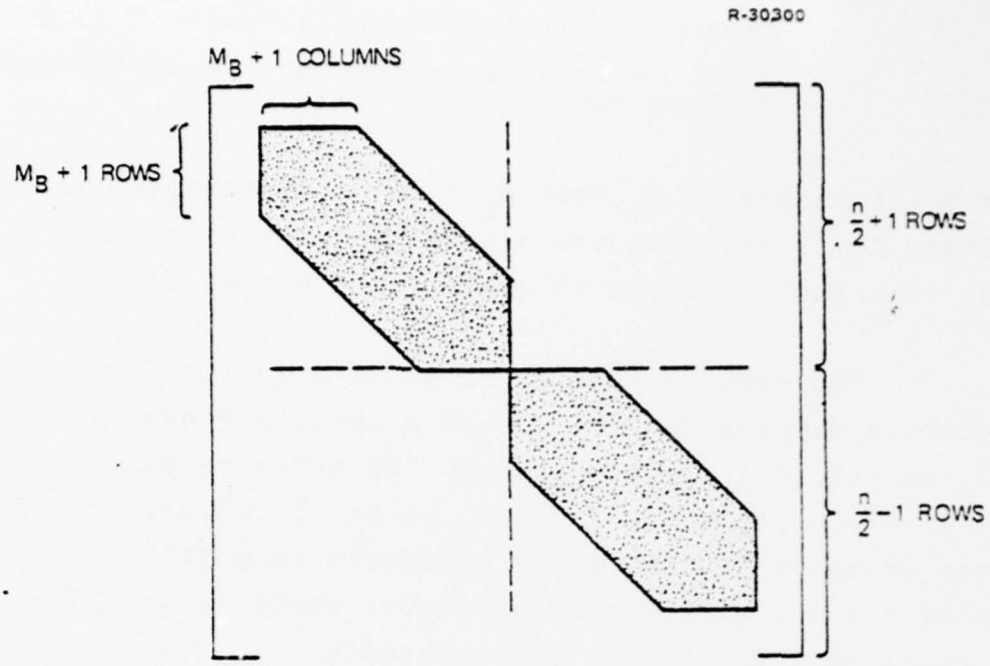

Figure 2.3-4 Structure of Discrete Spectral Density Under Sine-Cosine Transformation

the solution, due to the neglected out-of-band elements in T' is controlled by adjusting the matrix bandwidth of T_δ, with a complementary change in the data window function as described below. Bounds on the computational error arising from this source are presented here.

The computational details of the banded Cholesky decomposition algorithm are provided in Ref. 12. Only two features of the algorithm are important to the present application:

- The banded Cholesky algorithm is an exact procedure (within numerical error) for solving a system of equations with banded structure of the form of Eq. 2.3-5.

- The number of numerical operations required is approximately $C(M_B+1)^2 n$, where C is a small constant dependent on the particular implementation.

For small values of M_B (say $M_B < 25$) the numerical work of solving Eq. 2.3-2 with the banded Cholesky procedure is actually less than that required to compute the elements of T_δ.

The error bounds given in this section are parameterized by a damping factor, δ, and a resulting quantity which will be called data de-emphasis. In order to guarantee that the error in replacing T' by T_δ in Eq. 2.3-2 produces a small error in the solution, it is necessary to modify T' by introducing a small amount of ficticious, white noise. The system of equations, Eq. 2.3-2, is replaced by

$$(T' + \delta I)\underline{u}' = \underline{z}' \qquad (2.3\text{-}11)$$

When Eq. 2.3-11 is solved by Cholesky decomposition T' is approximated by T_δ and Eq. 2.3-11 becomes

$$(T_\delta + \delta I)\underline{u}'' = \underline{z}' \qquad (2.3\text{-}12)$$

The number δ is a small constant which can be chosen to trade off computational effort for computational error. The modification represented by Eqs. 2.3-11 and 2.3-12 is necessary because of the very small eigenvalues introduced in T' by the use of highly tapered data windows. It can be shown that the square of the smallest weight in the data window is an upper bound to the smallest eigenvalue of T'. These small eigenvalues introduce very large eigenvalues in $(T')^{-1}$, which greatly amplify the error $(\underline{u}'-\underline{u}'')$ due to the difference between T' and T_δ. That is, the system of Eq. 2.3-2 is

ill-conditioned* when windows are used. By contrast, the matrices $T' + \delta I$ and $T_\delta + \delta I$ can have no eigenvalues smaller than δ so that Eqs. 2.3-11 and 2.3-12 are well-conditioned. The actual impact of this modification on the error ($\underline{u}'-\underline{u}''$) is reflected in the error bounds presented in this section.

The modification of T' represented by Eq. 2.3-11 has an important interpretation in terms of the original estimation problem. The original system of equations involving T', Eq. 2.3-2, is simply the transform of the covariance equations. Eq. 2.3-1. By inverting the transformation process, the system of covariance equations corresponding to Eq. 2.3-11 is found to be

$$(T + D)\,\underline{u} = \underline{z} \tag{2.3-13}$$

where D is the diagonal matrix

$$D = \delta\ \mathrm{diag}\ (w_0^{-2},\ w_1^{-2},\ \ldots,\ w_{n-1}^{-2}) \tag{2.3-14}$$

Equation 2.3-13 shows that the addition of a multiple of the identity matrix to T' corresponds to the addition of the same multiple of the inverse of the window matrix squared to T. This may be interpreted as a model for the addition of uncorrelated measurement noise to the data. (Note that no noise is actually added to the data.) The variance of this additional noise changes with location along the data track in proportion to the square of the inverse of the window function. The variance of the added noise, which is large near the ends of the track, and small near the center, is called the data de-emphasis function and is displayed in Fig. 2.3-5 for a typical Kaiser data window.

---

*Ill-conditioning is discussed in Ref. 20 and Appendix B.

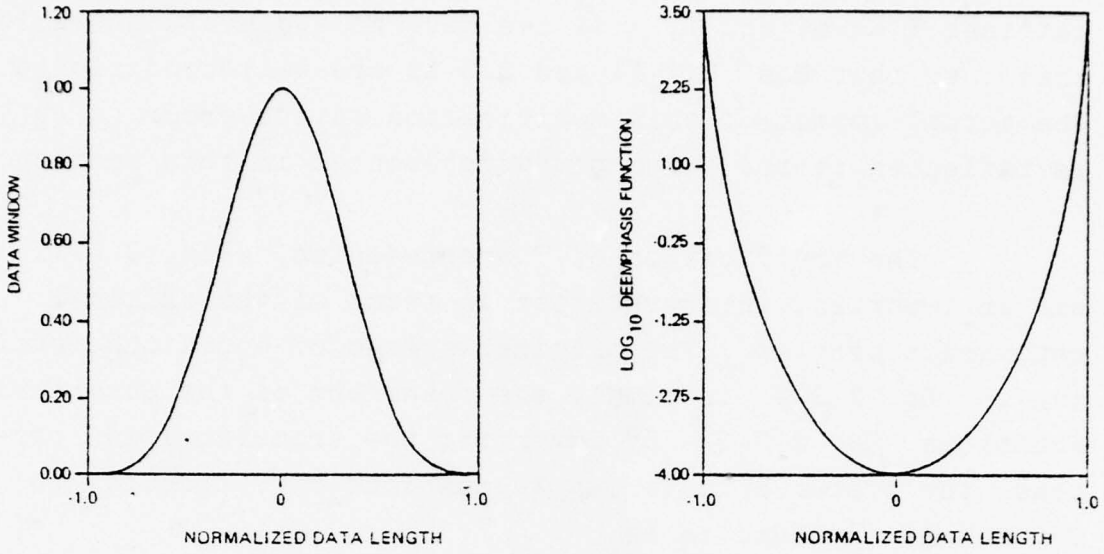

Figure 2.3-5 Data Window and Resulting De-Emphasis (Kaiser Window, M_B=6, δ=10^{-4}, n=128)

The modification represented by Eqs. 2.3-11 and 2.3-13 changes the estimation problem which is actually solved by the numerical algorithm. In the modified problem the quality of the data is gradually de-emphasized as the ends of the data track are approached. Points along the track, for which the signal-to-noise ratio

$$S_k = \frac{T_{kk}}{D_{kk}} \qquad (2.3\text{-}15)$$

is less than one, may be regarded as having been lost due to the introduction of computational data de-emphasis. The fractional number of data points for which S_k is less than one defines a performance index, the data de-emphasis index, which is associated with a given damping factor, δ, and a given window function. The data de-emphasis resulting from a number of combinations of damping factor and matrix bandwidth is presented in Fig. 2.3-6.

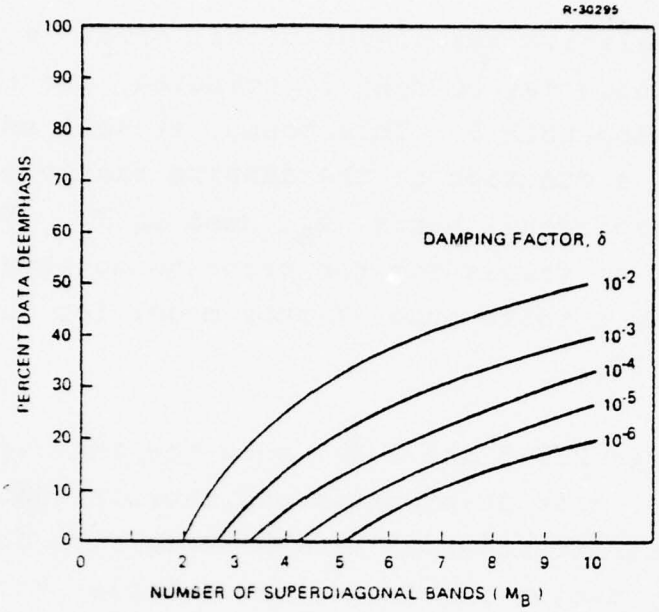

Figure 2.3-6 Data De-Emphasis Resulting from Computational Damping

An important concern in the use of an approximate method to compute estimates from data is the expected increase in estimation error due to the computational error. In the case of the band-diagonal method for solving covariance equations, computational error in the estimate arises because the error vector

$$\delta \underline{u} = \underline{u}' - \underline{u}'' \tag{2.3-16}$$

is, in general, nonzero. Since the data vector $\underline{z}$ is a random quantity, $\delta \underline{u}$ and the resulting increase in estimation error, $\delta \hat{\underline{x}}$, are also random. The magnitude of this error can be measured by the ratio*

$$\varepsilon = \left[\frac{E(\delta \hat{\underline{x}}^T \, \delta \hat{\underline{x}})}{E(\hat{\underline{x}}^T \, \hat{\underline{x}})} \right]^{\frac{1}{2}} \tag{2.3-17}$$

*E denotes the ensemble expectation operator.

which is the relative rms computational error in $\hat{\underline{x}}$. A realistic upper bound, which may be readily computed, for the quantity ε is derived in Appendix B. This bound, as well as the actual value of ε, is a function of the damping factor δ and the number of superdiagonal bands, M_B, used in T_δ. Figure 2.3-7 presents a set of values for the error bound obtained when T is generated by a third order Markov model for the gravity anomaly (Ref. 13).

Figures 2.3-6 and 2.3-7 show the two major measures of performance, data de-emphasis and computational error, as a function of matrix bandwidth M_B, which in turn determines the amount of computation required. For example, with seven superdiagonal bands and a damping factor of 10^{-4} the error bound is 0.1%. The resulting data de-emphasis is about 22%. It is possible to achieve the same error bound with a damping factor of 10^{-6} by using nine superdiagonal bands and performing more computation. In this case the data de-emphasis is reduced to 17%. There is thus a tradeoff, controlled by the damping factor, between data de-emphasis and computational effort. A given level of computational accuracy may be obtained with as small a level of data de-emphasis as desired, at the expense of a larger matrix bandwidth and increased computing time. The effect on computational error and data de-emphasis of reducing the damping factor is demonstrated in Fig. 2.3-8.

2.4 APPLICATION DISCUSSION

To provide perspective on the use of GEOFAST, a sample application to gravity gradiometer data is outlined. For simplicity the example treats only one of the five independent elements of the gravity gradient tensor. In most actual applications, however, all of the measured gradients would be

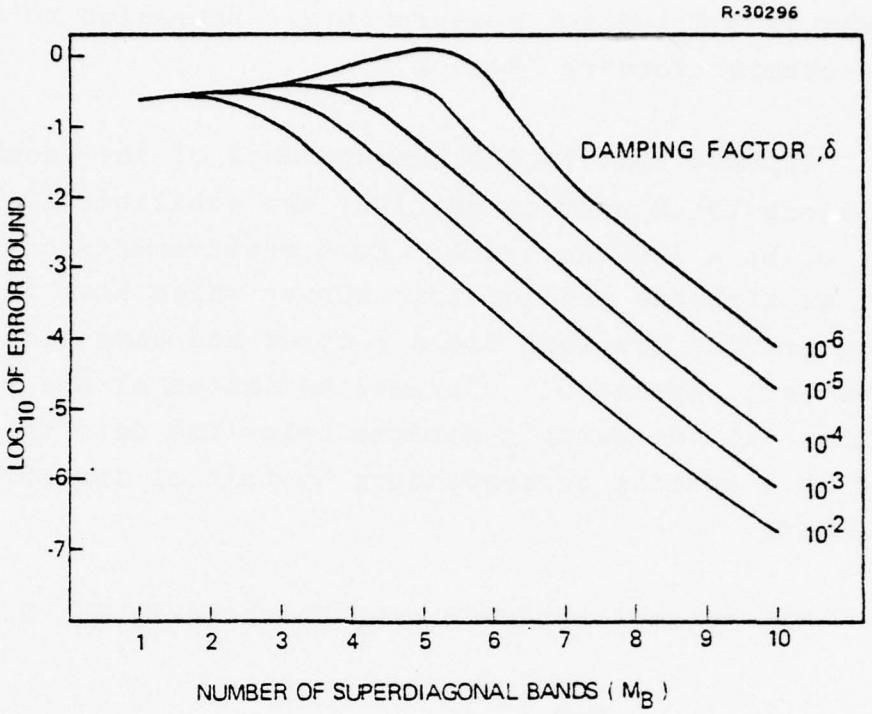

Figure 2.3-7 Relative RMS Computational Error for Band Diagonal Method

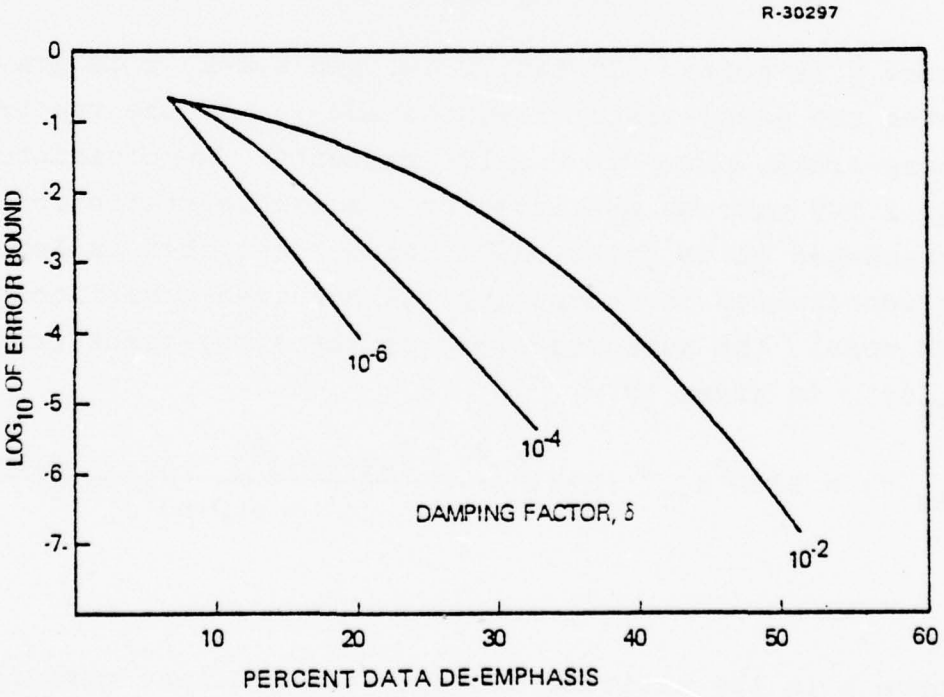

Figure 2.3-8 Computational Error and Data De-Emphasis Regimes for Various Damping Factors

processed as multisensor measurements. Extension to many sensors is straightforward (Ref. 1).

Suppose that 10,000 measurements of the anomalous, along-track, along-track gravity gradient are available at 0.1 km intervals, i.e. on a 1000 km track. Such measurements could be the outputs of an airborne gradiometric survey which have the reference spheroid gravity gradient field removed and have been prefiltered (e.g. averaged). Optimal estimates of the vertical deflection, at the earth's surface below the data track are desired at a spacing corresponding to that of the airborne measurements.

The optimal estimate of $\underline{\xi}$ is given by Eq. 2.1-2 where

$$\underline{\hat{x}} = \underline{\hat{\xi}} \tag{2.4-1}$$

$$\underline{z} = \frac{1}{g}\,\underline{\gamma}_{\tau\tau} + \underline{v} \tag{2.4-2}$$

where $\underline{v}$ is noise. In Eqs. 2.4-1 and 2.4-2, g is gravity, τ denotes the along-track direction and $\underline{\gamma}_{\tau\tau}$ is the vector of anomalous along-track, along-track self-gradients. The covariance matrices of Eq. 2.1-2 must be specified by a suitable statistical model. The attenuated white noise (AWN) model, described in Refs. 1 and 21, is appropriate for computing the required covariances. Using the AWN model, the autocovariance of the along-track gradient, $C_{zz}(\tau)$, is given by

$$C_{zz}(\tau) = 128D^6\sigma_{\tau\tau}^2\,(D+h)\frac{7\tau^2\,[\tau^2-8(D+h)^2] + [\tau^2+4(D+h)^2]^2}{[\tau^2+4(D+h)^2]^{11/2}} + R \tag{2.4-3}$$

where h is the altitude at which the gradient measurements are

taken, τ is the shift distance and R is the measurement error covariance matrix. The model parameters, $\sigma_{\tau\tau}$ (the rms along-track, along-track gradient) and D (a measure of the rate-of-decrease of the autocovariance function), are determined by statistical analysis of the data as described in Ref. 21. Typical values to be expected are 24 EU* and 35 km respectively. The cross covariance between the anomalous, along-track, along-track self-gradient at altitude, h, and the along-track gravity disturbance on the ground is given by the AWN model as

$$C_{xz}(\tau) = \frac{64}{3}\tau D^6 \sigma_{\tau\tau}^2 (2D+h) \frac{7\tau^2 [\tau^2 - 2(2D+h)^2] + [\tau^2 + (2D+h)^2]^2}{[\tau^2 + (2D+h)^2]^{11/2}} \qquad (2.4\text{-}4)$$

The elements of the matrices C_{zz} and C_{xz} are given by

$$\left[C_{zz}\right]_{jk} = C_{zz}(\tau_{jk}) \qquad (2.4\text{-}5)$$

$$\left[C_{xz}\right]_{jk} = C_{xz}(\tau_{jk}) \qquad (2.4\text{-}6)$$

$$\left[\tau_{jk}\right] = (k-j)\Delta \qquad j, k = 1, 2 \ldots 10{,}000 \qquad (2.4\text{-}7)$$

and Δ is the data spacing, 0.1 km. The indices j and k are data element counters.

In principle, Eq. 2.1-2 could now be solved directly for the desired deflection estimates. However, in practice, the 10,000 x 10,000 dimensionality of C_{zz} would make the C_{zz}^{-1} operation computationaly prohibitive. In addition, premultiplication of C_{zz}^{-1} by C_{xz} would be exceedingly burdensome.

The initial operation of the GEOFAST algorithm is to multiply the data vector, element-by-element, by the Kaiser

*1.0 EU = 0.1 mgal/km = 10^{-9} sec^{-2}

window exemplified in the lower right graph of Fig. 2.3-2.* Note that in the windowing operation, as with all of the operations involved in GEOFAST, the count of scalar arithmetic procedures is of the order of the number of elements in the data vector (except FFTs which go as n log n). Following windowing, the gradiometer data is fast Fourier transformed into the "intermediate" frequency domain data vector, $\underline{z}$.

The transform of the Kaiser window function, $\underline{\Omega}$, is computed by Eq. 2.2-21, an operation involving a FFT and scaling. The "window shape" variable, M_B, is chosen from Fig. 2.3-7 to provide acceptable accuracy and reasonable computation time. Note that the choice of M_B specifies the number of bands which are ultimately retained in the matrix inverse computation. When M_B is selected, the value of the data de-emphasis damping factor, δ, is also chosen from Fig. 2.3-8. Transformation of, $\underline{\Omega}$, by the matrix H (given by Eq. 2.3-10) follows, i.e.

$$\underline{\Omega}_H = H\,\underline{\Omega} \qquad (2.4\text{-}8)$$

The circulant vector $\underline{c}$ (first column of the circulant matrix, C) is formed using Eq. 2.2-10. The first 10,000 elements, c_ℓ, are given by the AWN model along-track self-gradient covariance function of Eqs. 2.4-3 and 2.4-5 with j=1 and k = 1, 2 ... 10,000. The FFT of $\underline{c}$ is computed using Eq. 2.2-23 which provides the elements of the gradient auto-spectrum $\underline{\tau}$. Equation 2.3-6 is now invoked to compute the M_B diagonal band elements, $\left[T_\delta\right]_{k,\,k+m}$, which will be supplied to the inverse calculation. In the application of Eq. 2.3-6 the Ω_ℓ elements used are taken

*In Fig. 2.3-2 only half of the window is depicted. In actual fact, the Kaiser window is symetric over the data interval and weights data in the center most heavily.

from the transformed window function vector, $\underline{\Omega}_H$. To the main diagonal elements of T_δ, the value of the data de-emphasis factor, δ, chosen at the outset, is now added.

The equation set

$$T_\delta \, \underline{u}' = \underline{z}' \tag{2.4-9}$$

where T_δ is banded diagonal and $\underline{z}'$ the windowed, transformed gradient data vector, is now completely specified. Application of the banded-Cholesky decomposition routine to Eq. (2.4-9) provides the "intermediate solution" vector $\underline{u}'$.

To prepare the vector $\underline{u}'$ for the fast multiplication portion of the estimation process (i.e., accounting for the elements of the cross correlation between gradients and deflections, C_{xz}) the transformation given by Eqs. 2.3-3 and 2.3-9 must be applied, namely,

$$\underline{b} = WF^{\top}H^{\top}\underline{u}' \tag{2.4-10}$$

Since the window matrix, W, is diagonal and $H^{\top}$ has a sparse structure similar to that of H, Eq. 2.4-10 is easily implemented without adverse effect on the efficiency of GEOFAST.

The vector, $\underline{b}$, is the solution to the inverse portion of the problem. Fast multiplication is now used to obtain the matrix product $C_{xz}\,\underline{b}$. The gradient-deflection cross covariance matrix definitions of Eqs. 2.4-3 and 2.4-6 are used provide elements for the circulant vector, $\underline{c}$, of Eq. 2.2-10. Equation 2.2-10 is applied to C_{xz} in the same fashion as previously accomplished for C_{zz} in the inversion portion of GEOFAST. The vector $\underline{c}$ undergoes the FFT operation as indicated in Eq. 2.2-13a to

provide $\underline{\Phi}_c$. The solution vector, $\underline{b}$, to the inverse portion of the problem is augmented with zeros and fast Fourier transformed by Eq. 2.2-13b. The result, $\underline{B}$, is multiplied element-by-element by $\underline{\Phi}_c$ and scaled as indicated in Eq. (2.2-15). This result is inverse Fourier transformed to complete the estimation procedure. The first 10,000 elements of the inverse transform are the desired along-track vertical deflection estimates, $\hat{\underline{\xi}}$. It is appropriate to emphasize that the deflection estimation problem outlined above was chosen only for conceptual clarity. The actual solution of this problem would not pose a severe test of GEOFAST's capabilities.

3. CONCLUSIONS AND RECOMMENDATIONS

In Ref. 1, TASC derived a frequency domain algorithm for efficiently processing gravimetric sensor data. This report presents significant alterations to the algorithm based upon explicit compensation for the adverse computational effects resulting from the finite length of gravimetric data records. Using the new algorithm the accuracy of gravity quantity estimates is improved without noticable sacrifices in computer speed. As a result, the enhanced algorithm, GEOFAST, is applicable to a very broad class of gravity quantity estimation problems.

The keynote of GEOFAST is judicious application of fast Fourier transform techniques. However, since these techniques exploit certain mathematical structures, the gravity data and the associated covariance models must exhibit these structural forms. The requirements are

- Input data must be regularly spaced on a Cartesian grid. If the original data not rectangularly gridded it can be converted by an appropriate preprocessing stage involving averaging or interpolation.
- Stationary, self-consistent statistical gravimetric models must be used.

Currently the algorithm is formulated in terms of estimation along and above a one-dimensional survey track. Preliminary investigation suggests that extension to a two-dimensional region can be accomplished without fundamental difficulty but will involve considerable attention to mathematical details. Prior to such extension, it is recommended

that a range of tests be conducted which exercise the algorithm with both simulated and real gravimetric data. The purpose of the tests is to

- Validate the algorithm by performing several "end-to-end" checks
- Establish performance for very large data samples
- Verify theoretical estimates of accuracy and computer speed
- Identify possible sources of numerical ill-conditioning or dynamic range limitation.

The new algorithm, when fully tested, can be expected to provide a mature tool for estimating gravity field quantities from data.

APPENDIX A

THE TRANSFORM OF A WINDOWED TOEPLITZ MATRIX

Consider an n×n Toeplitz matrix T with elements

$$[T]_{jk} = t_{k-j} \quad 0 \leq j, k \leq n-1 \tag{A-1}$$

corresponding to the function t_ℓ where $-(n-1) \leq \ell \leq (n-1)$. Let the window function w_ℓ be given for $0 \leq \ell \leq n-1$, and define the n×n matrix

$$w = \text{diag}\,(w_0, w_1, \ldots, w_{n-1}) \tag{A-2}$$

A windowed Toeplitz matrix is a matrix of the form WTW. The Discrete Fourier Transform (DFT) of such a matrix is given by

$$T_\omega = F_n W T W F_n^+ \tag{A-3}$$

where

$$[F_n]_{jk} = \frac{1}{\sqrt{n}} \exp -\frac{2\pi ijk}{n}, \quad 0 \leq j, k \leq n-1 \tag{A-4}$$

is the n-dimensional DFT matrix.* The purpose of this appendix is to derive a computationally efficient formula for T_ω by expression it in terms of a circulant matrix.

---

*The symbol i stands for $\sqrt{-1}$ and $^+$ indicates complex conjugate transpose.

A circulant matrix (Ref. 8) is a Toeplitz matrix C with $t_{-\ell} = t_{n-\ell}$. The fundamental property of circulant matrices is that they are diagonalized by the DFT. That is,

$$F_n \, C F_n^{\dagger} = \text{diag}\,(\underline{d}) \tag{A-5}$$

$$\underline{d} = \sqrt{n}\, F_n^{\dagger}\, \underline{t} \tag{A-6}$$

If C is a real symmetric matrix then its eigenvalues, d_ℓ, are real and Eqs. A-5 and A-6 hold with F_n and $F_n^{\dagger}$ interchanged. Also if $\underline{d}$ defines an arbitrary diagonal matrix then its transform is a circulant C. These properties are used below.

The matrix T is extended to a 2n×2n circulant matrix $\tilde{T}$ by the definitions

$$[\tilde{T}]_{jk} = c_{k-j} \quad 0 \le j,\, k \le 2n-1 \tag{A-7}$$

where

$$c_\ell = \begin{cases} t_\ell & 0 \le \ell \le n-1 \\ 0 & \ell = n \\ t_{\ell-2n} & n+1 \le \ell \le 2n-1 \end{cases} \tag{A-8}$$

and $c_{-\ell} = c_{2n-\ell}$ for $1 \le \ell \le 2n-1$. The matrix $\tilde{T}$ has the partitioned form

$$\tilde{T} = \begin{bmatrix} T & T' \\ T' & T \end{bmatrix} \tag{A-9}$$

where T' is a Toeplitz matrix corresponding to the function

$$t'_\ell = \begin{cases} t_{\ell-n} & \ell > 0 \\ 0 & \ell = 0 \\ t_{\ell+n} & \ell < 0 \end{cases} \tag{A-10}$$

A 2n×2n extended version of W is defined by

$$W = \begin{pmatrix} W & 0 \\ 0 & 0 \end{pmatrix} \tag{A-11}$$

The windowed Toeplitz matrix WTW may now be expressed in terms of the diagonal matrix $\tilde{W}$ and the circulant matrix $\tilde{T}$ by

$$\begin{pmatrix} WTW & 0 \\ 0 & 0 \end{pmatrix} = \tilde{W}\tilde{T}\tilde{W} \tag{A-12}$$

Introducing the n×2n sampling matrix S defined by

$$S = \begin{pmatrix} 1 & 0 & . & . & . & 0 \\ 0 & 0 & 1 & . & . & 0 \\ & & & & & . \\ & & & & & . \\ & & & & & . \\ . & . & . & 0 & 1 & 0 \end{pmatrix} \tag{A-13}$$

it may be verified that

$$T_\omega = SF_{2n}\ \tilde{W}\tilde{T}\tilde{W}\ F_{2n}^{\dagger}S^{T} \tag{A-14}$$

where F_{2n} is the 2n×2n Discrete Fourier Transformation defined by Eq. A-4 with n replaced by 2n. Equation A-14 expresses T_ω as the result of sampling every other row and column of a matrix which is the transform of a product of diagonal window matrices and a circulant matrix.

The application of the circulant properties stated above produces the desired expression for T_ω. Equation A-14 may be written as

$$T_\omega = S\, \tilde{W}_\omega \tilde{T}_\omega \tilde{W}_\omega S^T \tag{A-15}$$

where $\tilde{W}_\omega$ and $\tilde{T}_\omega$ are the transformed matrices

$$\tilde{W}_\omega = F_{2n}\, \tilde{W}\, F_{2n}^{\dagger} \tag{A-16}$$

$$\tilde{T}_\omega = F_{2n}\, \tilde{T}\, F_{2n}^{\dagger} \tag{A-17}$$

Taking the conjugate of Eqs. A-5 and A-6 shows that the first of these matrices is a circulant, with the elements

$$\left[\tilde{W}_\omega\right]_{jk} = \Omega_{k-j},\ 0 \le j,\ k \le 2n-1 \tag{A-18}$$

where Ω_ℓ is given by the transform

$$\left(\Omega_0,\ \Omega_1,\ \ldots,\ \Omega_{2n-1}\right)^T = \underline{\Omega} = \frac{1}{\sqrt{2n}}\, F_{2n}^{\dagger} \begin{pmatrix} \underline{w} \\ \underline{0} \end{pmatrix} \tag{A-19}$$

and $\underline{w}$ is the n-vector defined by the window function

$$\underline{w} = (w_0,\ w_1,\ \ldots,\ w_{n-1})^T \tag{A-20}$$

It also follows directly from Eqs. A-5 and A-6 that the matrix $\tilde{T}_\omega$ of Eq. A-17 is diagonal, of the form

$$\tilde{T}_\omega = \mathrm{diag}\,(\tau_0,\ \tau_1,\ \ldots,\ \tau_{2n-1}) \tag{A-21}$$

where $\underline{\tau} = (\tau_0,\ \tau_1,\ \ldots,\ \tau_{2n-1})^T$ is defined by the vector $\underline{c}$ of Eq. A-8 via

$$\underline{\tau} = \sqrt{2n}\, F_{2n}\, \underline{c} \tag{A-22}$$

The expression of Eq. A-15, together with the special forms for $\tilde{W}_\omega$ and $\tilde{T}_\omega$ described by Eqs. A-18 and A-21, is the basic result of this appendix in matrix form.

A useful element-by-element formula for T_ω is a consequence of Eq. A-15. Substitution of the definitions from Eqs. A-13, A-18, and A-21, with some simplification, produces the expression*

$$\left[T_\omega\right]_{jk} = \sum_{\ell=0}^{2n-1} \Omega_{\ell-2j}\, \bar{\Omega}_{\ell-2k}\, \tau_\ell \qquad \text{(A-23)}$$

where Ω_ℓ is the transform of the window function, Eq. A-19, and τ_ℓ is the power spectrum of $\tilde{T}$, defined by Eq. A-22. Equation A-23 provides a computationally efficient formula for the calculation of T_ω.

*The symbol $\bar{\Omega}_\ell$ represents the complex conjugate of the quantity Ω_ℓ.

APPENDIX B

ESTIMATION ERROR BOUNDS

In this appendix an error bound is derived for least squares estimation using an approximate measurement covariance matrix. This bound is particularly useful in the design and analysis of fast estimation techniques. Furthermore the bound is relatively easy to compute in terms of known matrices. The result is closely related to well-known error bounds for deterministic linear systems (Ref. 12, Section 8 and Ref. 20, Chapter 2). The derivation assumes that all matrices are real but readily extends to complex matrices if "transpose" is replaced by "conjugate transpose."

Consider the least squares estimate

$$\underline{\hat{x}} = C_{xz}\, C_{zz}^{-1}\, \underline{z} \qquad \text{(B-1)}$$

where $\underline{z}$ is the measurement vector of dimension n, C_{zz} is the measurement covariance matrix, $\underline{x}$ is the estimate vector of dimension m, and C_{xz} is the cross-covariance between $\underline{x}$ and $\underline{z}$. An approximate covariance matrix

$$C_{\hat{\delta}} = C_{zz} + \delta C \qquad \text{(B-2)}$$

is constructed and used to obtain an approximate estimate

$$(\underline{\hat{x}} + \delta\underline{\hat{x}}) = C_{xz}\, C_{\hat{\delta}}^{-1}\, \underline{z} \qquad \text{(B-3)}$$

It follows that

$$\delta\hat{\underline{x}} = -C_{xz}(I-C_{\delta}^{-1}C_{zz})C_{zz}\underline{z} \tag{B-4}$$

where the matrix

$$R = I - C_{\delta}^{-1}C_{zz} \tag{B-5}$$

is called the residual matrix. Since $\underline{x}$ and $\underline{z}$ are random variables an appropriate error measure is the relative rms error given by

$$\varepsilon = \left\{\frac{E[\delta\hat{\underline{x}}^T\delta\hat{\underline{x}}]}{E[\hat{\underline{x}}^T\hat{\underline{x}}]}\right\}^{\frac{1}{2}} \tag{B-6}$$

where E denotes the ensemble expectation operator.

Introducing the matrix trace operator, Tr, and using

$$E\,[\underline{z}\underline{z}^T] = C_{zz} \tag{B-7}$$

$$E\,[\underline{x}^T\underline{x}] = Tr\ E[\underline{x}\underline{x}^T] \tag{B-8}$$

the following expressions are obtained.

$$E\,[\delta\hat{\underline{x}}^T\delta\hat{\underline{x}}] = Tr\left\{C_{xz}RC_{zz}^{-1}R^TC_{sz}^T\right\} \tag{B-9}$$

$$E\,[\hat{\underline{x}}^T\hat{\underline{x}}] = Tr\left\{C_{xz}C_{zz}^{-1}C_{xz}^T\right\} \tag{B-10}$$

Since C_{zz} is positive definite it has a unique symmetric square root $C_{zz}^{\frac{1}{2}}$ and Eq. B-9 may be rewritten

$$E\left[\delta\hat{\underline{x}}^T\delta\hat{\underline{x}}\right] = \mathrm{Tr}\left\{C_{xz}C_{zz}^{-\frac{1}{2}}\tilde{R}^2C_{zz}^{-\frac{1}{2}}C_{xz}^T\right\} \tag{B-11}$$

where the matrix

$$\tilde{R} = C_{zz}^{+\frac{1}{2}}RC_{zz}^{+\frac{1}{2}} = I - C_{zz}^{\frac{1}{2}}C^{-1}C_{zz}^{\frac{1}{2}} \tag{B-12}$$

is a symmetric form of the residual matrix.

Two properties of the trace operator are needed to complete the derivation. The first is the identify $\mathrm{Tr}\{AB\} = \mathrm{Tr}\{BA\}$ and the second the inequality

$$\mathrm{Tr}\{AB\} \leq \|A\|_2 \ \mathrm{Tr}\{B\} \tag{B-13}$$

where the euclidean matrix norm* is defined by

$$\|A\|_2 = \sqrt{\lambda_{max}(A^TA)} \tag{B-14}$$

and $\lambda_{max}(B)$ denotes the maximum eigenvalue of B. Applying these two properties to Eq. B-11 leads to the result

$$E\left[\delta\hat{\underline{x}}^T\delta\hat{\underline{x}}\right] \leq \|\tilde{R}^2\|_2 \ \mathrm{Tr}\left\{C_{xz}C_{zz}^{-1}C_{xz}^T\right\} \tag{B-15}$$

Combining Eqs. B-6, B-10, and B-15 with the equality $\|\tilde{R}^2\|_2 = \|\tilde{R}\|_2^2$ the final bound becomes simply

$$\varepsilon \leq \|\tilde{R}\|_2 \tag{B-16}$$

---

*For a general discussion of matrix norms and their properties see Ref. 20, Chapter 1 and Ref. 12, Section 2.

The error bound in Eq. B-16 is awkward to compute since it involves the square root $C_{zz}^{\frac{1}{2}}$ and the eigenvalues of $\tilde{R}$ through Eq. B-14. For a symmetric matrix A, a simpler relation can be written

$$\|A\|_2 = |\lambda_{max}(A)| \leq \|A\|_1 \qquad \text{(B-17)}$$

where the L_1 matrix norm is defined by

$$\|A\|_1 = \max_j \sum_{i=1}^{n} |a_{ij}| \qquad \text{(B-18)}$$

and a_{ij} are the elements of A (Ref. 20). It follows that a simpler error bound is

$$\varepsilon \leq \|P \tilde{R} P^{-1}\|_2 \leq \|P \tilde{R} P^{-1}\|_1 \qquad \text{(B-19)}$$

where P is an arbitrary non-singular matrix which may be chosen to minimize the bound.

A useful choice of P in Eq. B-19 is $P = D^{\frac{1}{2}} C_{zz}^{-\frac{1}{2}}$, where D is a diagonal matrix, since it leads to

$$\varepsilon \leq \|D^{\frac{1}{2}} R D^{-\frac{1}{2}}\|_1 \qquad \text{(B-20)}$$

which requires only the computation of the residual matrix R, plus row and column scaling.* For the norm in Eq. B-18 it is desirable to "balance" the matrix so that all (absolute) column sums are nearly equal. This is accomplished approximately by defining the diagonal matrix D to consist of the diagonal elements of C_ζ.

*Scaling to reduce matrix norms is discussed in Ref. 12, Section 11.

For illustration, suppose that C is obtained from C_{zz} by striking out the off-diagonal elements. (In the fast estimation algorithm C is constructed to be band diagonal.) Then since C_{zz} is a covariance matrix

$$\| D^{\frac{1}{2}} R D^{-\frac{1}{2}} \|_1 = \| I - C_\delta^{-\frac{1}{2}} C_{zz} C_\delta^{-\frac{1}{2}} \|_1$$

$$= \max_j \sum_{i=1}^{n} |r_{ij}| \quad (i \neq j) \tag{B-21}$$

where the r_{ij} are correlation coefficients. Thus the column sums in Eq. B-21 are all of the same order of magnitude and bounded by (n-1).

Interestingly, the error bounds in Eqs. B-16 and B-20 are the same as for the relative error in a deterministic linear system. Also the dependence of the error on the condition of the matrix C_δ is easily obtained. For example, set $P = C_{zz}^{-\frac{1}{2}}$ in Eq. B-19 and the bound can be written (see Eq. B-2)

$$\varepsilon \leq \|R\|_2 = \|C_\delta^{-1} \delta C\|_2 \leq \kappa_2(C_\delta) \frac{\|\delta C\|_2}{\|C_\delta\|_2} \tag{B-22}$$

where

$$\kappa_2(C_\delta) = \|C^{-1}\|_2 \|C_\delta\|_2 = \lambda_{max}(C_\delta)/\lambda_{min}(C_\delta) \tag{B-23}$$

is the condition number of C_δ in the euclidean norm.

REFERENCES

1. Thomas, S.W. and Heller, W.G., "Efficient Estimation Techniques for Integrated Gravity Data Processing," The Analytic Sciences Corporation, Report No. AFGL-TR-76-0232, September 1976.

2. Heiskanen, W.A. and Moritz, H., Physical Geodesy, W.H. Freeman and Co., 1967.

3. Moritz, H., "Advanced Least-Squares Methods," Report No. 175, Dept. of Geod. Sci., Ohio State University, Columbus, Ohio, 1972.

4. Rapp, R.H. and Agajelu, S.I., "Comparison of Upward Continued Anomalies by the Poison Integral and by Collocation," Report No. 227, Dept. of Geod. Sci., Ohio State University, Columbus, Ohio, June 1975.

5. Nash, R.A., Jr., Kasper, J.F., Crawford, B.S., and Levine, S.A., "Application of Optimal Smoothing to the Testing and Evaluation of Inertial Navigation System and Components," IEEE Transactions on Automatic Control, Vol. AC-16, No. 6, December 1971, pp. 806-816.

6. Argentiero, P. and Lowry, B., "On Estimating Gravity Anomalies - A Comparison of Least Squares Collocation with Conventional Least Squares, Techniques," Bulletin Geodesique, Vol. 51, No. 2, 1977.

7. Gentry, D.C. and Nash, R.A., Jr., "A Statistical Algorithm for Computing Vertical Deflections Gravimetrically," J. Geophys. Res., Vol. 77, 1972, pp. 4912-4919.

8. Bellman, R., Introduction to Matrix Analysis, McGraw-Hill, New York, 1960.

9. Cooley, J.W., Lewis, P.A.W., and Welch, P.D., "The Fast Fourier Transform and Its Applications," Report No. RC-1743, IBM Watson Research Center, Yorktown Heights, New York, 1967.

10. Stockham, T.G., "High-Speed Convolution and Correlation," 1966 Spring Joint Computer Conference, AFIPS Proc, Vol 28, pp. 228-233.

REFERENCES (Continued)

11. Gikhman, I.I. and Skorokhod, A.V., Introduction to the Theory of Random Processes, Saunders, Philadelphia, 1965.

12. Forsythe, G.E. and Moler, C.B., Computer Solution of Linear Algebraic Systems, Prentice-Hall, Englewood Cliffs, New Jersey, 1967.

13. Jordan, S.K., "Self-Consistent Statistical Models for the Gravity Anomaly, Vertical Deflections, and Undulation of the Geoid," J. Geophys. Res., Vol. 77, 1972, pp. 3660-3670.

14. Pratt, W.K., "Generalized Wiener Filter Computation Techniques," IEEE Trans. on Computers, Vol. C-21, July 1972, pp. 636-641.

15. Cooley, J.W. and Tukey, J.W., "An Algorithm for the Machine Calculation of Complex Fourier Series," Math. of Comp., Vol. 19, 1965, pp. 297-301.

16. Grenander, U. and Szego, G., Toeplitz Forms and Their Applications, Univ. of Calif. Press, Berkeley, California, 1958.

17. Rabiner, L.R. and Gold, B., Theory and Application of Digital Signal Processing, Prentice Hall, Englewood Cliffs, New Jersey, 1975.

18. Kaiser, J.F., "Nonrecursive Digital Filter Design using the I_0-SINH Window Function," Proc. 1974 IEEE Int. Symp. on Circuits and Syst., April 1974, pp. 20-23.

19. Gelb, A. (Ed.), Applied Optimal Estimation, M.I.T. Press, Cambridge, Massachusetts, 1974.

20. Isaacson, E. and Keller, H.B., Analysis of Numerical Methods, Wiley, New York, 1966.

21. Heller, W.G., "Self-Consistent Statistical Geodetic and Geophysical Error Models for Land-Based ICBMs," The Analytic Sciences Corp., Report No. TR-573-1, December 1975.